frontiers in Cell and Developmental Biology

REVIEW
published: 27 March 2020
doi: 10.3389/fcell.2020.00195

Current and Emerging Approaches for Studying Inter-Organelle Membrane Contact Sites

*Xue Huang, Chen Jiang, Lihua Yu and Aimin Yang**

School of Life Sciences, Chongqing University, Chongqing, China

Inter-organelle membrane contact sites (MCSs) are classically defined as areas of close proximity between heterologous membranes and established by specific proteins (termed tethers). The interest on MCSs has rapidly increased in the last years, since MCSs play a crucial role in the transfer of cellular components between different organelles and have been involved in important cellular functions such as apoptosis, organelle division and biogenesis, and cell growth. Recently, an unprecedented depth and breadth in insights into the details of MCSs have been uncovered. On one hand, extensive MCSs (organelles interactome) are revealed by comprehensive analysis of organelle network with high temporal-spatial resolution at the system level. On the other hand, more and more tethers involving in MCSs are identified and further works are focusing on addressing the role of these tethers in regulating the function of MCSs at the molecular level. These enormous progresses largely depend on the powerful approaches, including several different types of microscopies and various biochemical techniques. These approaches have greatly accelerated recent advances in MCSs at the system and molecular level. In this review, we summarize the current and emerging approaches for studying MCSs, such as various microscopies, proximity-driven fluorescent signal generation and proximity-dependent biotinylation. In addition, we highlight the advantages and disadvantages of the techniques to provide a general guidance for the study of MCSs.

Keywords: membrane contact sites, electron microscopy, super-resolution microscopy, FRET, proximity ligation assay, bimolecular fluorescence complementation, BioID, APEX

OPEN ACCESS

Edited by:
Du Feng,
Guangzhou Medical University, China

Reviewed by:
Thomas Becker,
University of Freiburg, Germany
Carmen Faso,
University of Bern, Switzerland

***Correspondence:**
Aimin Yang
aimin.yang@cqu.edu.cn

Specialty section:
This article was submitted to Molecular Medicine, a section of the journal Frontiers in Cell and Developmental Biology

Received: *20 January 2020*
Accepted: *09 March 2020*
Published: *27 March 2020*

Citation:
Huang X, Jiang C, Yu L and Yang A (2020) Current and Emerging Approaches for Studying Inter-Organelle Membrane Contact Sites. Front. Cell Dev. Biol. 8:195. doi: 10.3389/fcell.2020.00195

INTRODUCTION

A defining characteristic of eukaryotic cells is the presence of membrane-bound organelles surrounded by plasma membrane (PM). Inter-organelle membrane contact sites (MCSs) are classically defined as areas of close proximity between heterologous membranes. At MCSs, specific proteins (termed tethers) hold two organelles together and mediate the transfer of cytoplasmic materials between two organelles (**Table 1**; Helle et al., 2013; Eisenberg-Bord et al., 2016). The interest on MCSs has rapidly increased in the last few years, since MCSs have been involved in important cellular functions such as apoptosis, cell growth, organelle division and biogenesis

(Cohen et al., 2018; Scorrano et al., 2019). Emerging evidence suggests that MCSs play a crucial role in the transfer of cellular components between different organelles, which controls exchange of cellular signaling and regulates organelle membrane dynamics (Friedman et al., 2011; Prinz, 2014; Lahiri et al., 2015; Stefan et al., 2017). For instance, ER-mitochondria MCS is responsible for Ca^{2+} exchange and non-vesicular transfer of phospholipid between mitochondria and ER (Hayashi et al., 2009; Naon and Scorrano, 2014; Krols et al., 2016). The ER-related MCSs, including ER-mitochondria MCS and ER-PM MCS, contribute to autophagosome biogenesis (Hamasaki et al., 2013; Bockler and Westermann, 2014; Garofalo et al., 2016; Nascimbeni et al., 2017). The lysosome-related MCSs in eukaryotic cells act as a dynamic network for nutrient uptake, metabolic control, macromolecule degradation and signaling (Mc Donald and Krainc, 2017; Lawrence and Zoncu, 2019). Therefore, MCSs exist widely in cell and ensure signaling exchange and materials transfer between two different organelles (**Table 1**).

The dysfunction of MCSs has been implicated in neurodegenerative disorders and cancer (Prinz et al., 2020). To date, most investigations into the roles of MCSs dysfunction in disease have focused on ER-mitochondria MCSs (Paillusson et al., 2016). The mutation of the tether Mnd, VAPB or REEP defects ER-mitochondria MCS and Ca^{2+} signaling transfer, and finally leads to neurodegenerative disease (Vance et al., 1997; Nishimura et al., 2004; Schon and Area-Gomez, 2013; Stoica et al., 2014; Bernard-Marissal et al., 2015; Lim et al., 2015). In addition, the mutation of the tether BAP31 dysregulates ER-Golgi crosstalk and impacts Golgi apparatus, and thereby causing the X-link phenotype with deafness, dystonia and central hypomyelination (Cacciagli et al., 2013).

Electron microscopy (EM) provides the first evidence for the existence of sites of physical interaction between ER and mitochondria in the 1950s (Bernhard and Rouiller, 1956; Copeland and Dalton, 1959). Since then, however, the research on MCSs has been proceeded slowly due to lack of suitable study tools. From the early of 21st century, an unprecedented depth and breadth in insights into the details of MCSs have been uncovered gradually. On one hand, extensive MCSs (organelles interactome) are revealed by comprehensive analysis of organelle network with high temporal-spatial resolution at the system level (**Figure 1**). On the other hand, more and more tethers involving in MCSs are identified and further works are focusing on addressing the role of these tethers in regulating the function of MCSs at the molecular level (**Table 1**; Jansen et al., 2011; Elbaz-Alon et al., 2015; Jing et al., 2015; Kim et al., 2015; Besprozvannaya et al., 2018). These enormous progresses largely depend on the powerful approaches, including several different types of microscopies and various biochemical techniques (**Figure 1**). These approaches have greatly accelerated recent advances in MCSs at the molecular and system level (**Figure 2**). In this review, the current and emerging approaches for studying MCSs are summarized. In addition, the advantages and disadvantages of the approaches are highlighted to provide a general guidance for tool selection and optimization for the study of MCSs.

AN OVERVIEW OF THE APPROACHES FOR STUDYING MCSs

Visualization is a prerequisite for study of MCSs. The "membrane contact" was originated from an observation that topographical proximity between mitochondria and ER in cells of the pseudobranch gland of a teleost by EM (Bernhard and Rouiller, 1956; Copeland and Dalton, 1959). EM of cell specimen at the nanometer scale make observation of subcellular structures and MCSs possible. Recently, EM and its variants, such as focused ion beam-scanning EM (FIB-SEM) and electron tomography (ET), are widely employed to observe MCSs. High resolution of three-dimensional (3D) structure at ER-PM MCS in COS-7 cells was obtained by cryo-ET (Fernandez-Busnadiego et al., 2015). Meanwhile, various light microscopies based on fluorescence were developed in living cells. Confocal microscopy is used to visualize subcellular localization of fluorescent fusion membrane proteins and has been employed to reconstruct 3D imaging of ER-mitochondria juxtaposition as sites of Ca^{2+} transfer between both organelles in HeLa cells (Rizzuto et al., 1998). Lattice light-sheet microscopy (LLSM) was developed by using ultrathin light sheets from two-dimensional optical lattices to reveal organelle interactome at the systems-level in COS-7, HEK293 and MEF cells (Valm et al., 2017; D'Eletto et al., 2018). Super-resolution fluorescence microscopy (SRM) offers a unique window with extreme high temporal and spatial resolution for MCSs (Sydor et al., 2015; Sezgin, 2017; Jing et al., 2019). Recently, grazing incidence structured illumination microscopy (GI-SIM), one of SRM, was developed and applied to visualize ER-mitochondria MCS in COS-7 and U2OS cells (Guo Y. et al., 2018). In brief, various microscopies provide a large of direct evidence for visualization of MCSs and greatly facilitate the development of the field.

In combination of confocal microscopy, a variety of biochemical techniques, including proximity ligation assay (PLA) (Soderberg et al., 2006), fluorescence resonance energy transfer (FRET) (Csordas et al., 2010), bimolecular fluorescence complementation (BiFC) (Cabantous et al., 2005; Magliery et al., 2005) and dimerization-dependent fluorescent proteins (ddFP) (Alford et al., 2012a) were designed to observe and identify MCSs. These biochemical techniques are dependent on proximity-driven signal generation and amplification. Briefly, two fragments or proteins, fused with tethers or membrane proteins of different organelles, are each no signal or low signal on their own but are reconstituted to give strong signal when driven together by close membrane-membrane proximity. These techniques are widely employed to visualize MCSs and identify tethers involving in MCSs. In recent years, many studies focused on identification of new tethers. To achieve this purpose, two novel tools, BioID and APEX based on proximity-driven biotinylation were engineered and applied to identify new tethers and even systematically map MCSs in COS-7 and HEK293 cells (Hua et al., 2015; Cho et al., 2017).

Overall, these approaches have greatly accelerated research progress in MCSs (**Table 1** and **Figure 2**). It is expected that new approaches, such as SRM and proximity-driven biotinylation

TABLE 1 | Summary of membrane contact sites (MCSs).

Contact site	Date Of Discovery	Organism	Proposed function	Used Tools for MCSs	*Identified tethers*
ER-PM	1957 (Porter and Palade, 1957)	Mammalian	lipid transfer; activation of store-operated Ca^{2+} entry; autophagosome biogenesis	EM, ET, Confocal, FM, TIRFM	E-Syts (Schauder et al., 2014), GRAMD2a (Besprozvannaya et al., 2018), VAP-B-Nir2 (Kim et al., 2015), VAP-ORPs (Jansen et al., 2011), JPs (Takeshima et al., 2000; Landstrom et al., 2007), STIM1-Orail-hTRPC1 (Liou et al., 2007; Jardin et al., 2008)
		Yeast	membrane complex formation and localization	EM, FM, Confocal, FRET	Scs2-Scs22 (Manford et al., 2012), Tcb1/2/3 (Manford et al., 2012), Osh2/3 (Levine and Munro, 2001), Ist2 (Manford et al., 2012)
ER-Mitochondria	1959 (Copeland and Dalton, 1959)	Mammalian	Ca^{2+} exchange; lipid exchange; scission of mitochondria; autophagosome biogenesis	EM, FM, Confocal, PLA, FRET, SR-FACT	IP3R-GRP75-VDAC (Rizzuto et al., 1993; Szabadkai et al., 2006; D'Eletto et al., 2018), GRP75-TG2 (D'Eletto et al., 2018), BAP31-FIS1 (Iwasawa et al., 2011), Mfn2-Mfn2/Mfn1-Mfn2 (Naon et al., 2016), VAP-PTPIP51 (De Vos et al., 2012), Lam6 (Elbaz-Alon et al., 2015)
		Yeast(ERMES)	lipid exchange; phospholipid synthesis and cell growth; sterols transport	EM, FM, Confocal, SIM, TIRFM	ERMES complex (Kornmann et al., 2009; Kawano et al., 2018), Gem1 (Kornmann et al., 2011), Mmmr1 (Swayne et al., 2011), TOM5 (Lahiri et al., 2014), Lam6 (Elbaz-Alon et al., 2015), Ltc1-TOM70/71 (Murley et al., 2015), Num1 (Lackner et al., 2013)
ER-Endosome	2009 (Rocha et al., 2009)	Mammalian	sterol sensing and endosome positioning; cholesterol transfer; endosomal tubule fission regulation	EM, FM, Confocal, 3D-SIM, PLA, FRET	VAP-A-STARD3/STARD3NL (Alpy et al., 2013), VAP-A-ORP1L (Rocha et al., 2009), ORP5-NPC1 (Du et al., 2011), Protrudin (Raiborg et al., 2015), PTP1B-EGFR (Eden et al., 2010), Rab5 (Hsu et al., 2018), Spastin-IST1 (Allison et al., 2017), VAP-OSBP-PI4P (Dong et al., 2016), TMCC1-Coronin1C (Hoyer et al., 2018), PTP1B-G-CSFR (Palande et al., 2011)
ER-Golgi	1988 (Schweizer et al., 1988)	Mammalian	lipid exchange	EM, FM, Cryo-EM, Confocal, FRET	VAP-PI4P-OSBP (Mesmin et al., 2013; Jamecna et al., 2019), VAP-CERT (Hanada et al., 2003), VAP-FAPP2 (D'Angelo et al., 2007), VAP-Nir2 (Litvak et al., 2005)
		Yeast	ceramides transfer	EM, FM, APEX2	Nvj2 (Liu et al., 2017)
ER-LD	2006 (Robenek et al., 2006)	Mammalian	LD growth regulation	Confocal, SIM, APEX	Rab18-NRZ (NAG-RINT1-ZW10) (Xu et al., 2018)
		C. elegans	LD expansion	EM, Confocal	FATP1-DGAT2 (Xu et al., 2012)
		Drosophila	LD growth regulation	EM, ET, Confocal, LLSM	Seipin (Wang et al., 2016)
ER-Peroxisome	1987 (Yamamoto and Fahimi, 1987)	Mammalian	peroxisome growth; lipid homeostasis	SIM	VAPs-ACBD4 (Costello et al., 2017), VAPs-ACBD5 (Hua et al., 2017)
		Yeast	peroxisome growth	Confocal	Pex3-Inp1-Pex3 (Knoblach et al., 2013), Pex30 (Joshi et al., 2018)
ER-Lysosome	2018 (Atakpa et al., 2018)	Mammalian	Ca^{2+} exchange	TIRFM, STORM, LLSM, FIB-SEM	unknown
ER-Autophagosome	2016 (Wijdeven et al., 2016)	Mammalian	lipid transfer	Cryo-EM, Confocal, FRET	LTP-ATG2, VAP-A-ORP1L (Wijdeven et al., 2016)
ER-Vacuole	2000 (Pan et al., 2000)	Yeast	selectively sterols transport	FM, BiFC	Ltc1-Vac8 (Murley et al., 2015; Kakimoto et al., 2018), Nvj3-Mdm1 (Henne et al., 2015)
ER-DB	2020 (Dong et al., 2020)	Mammalian	unknown	SR-FACT	unknown

(Continued)

TABLE 1 | Continued

Contact Site	Date Of Discovery	Organism	Proposed Function	Used Tools for MCSs	Identified Tethers
Mitochondria-Golgi	2007 (Ouasti et al., 2007)	Mammalian	apoptosis related	TEM, FM	Fas (CD95/Apo1) (Ouasti et al., 2007)
Mitochondria-Lysosome	2002 (Ponka et al., 2002)	Mammalian	unknown	EM, Confocal, SIM, FRET, SR-FACT	unknown
Mitochondria-Endosome	2002 (Ponka et al., 2002)	Mammalian	early endosomal-mitochondrial contacts and transferrin uptake regulation	EM, FM, SR-FACT	Rab5 (Hsu et al., 2018)
Mitochondria-Peroxisome	2007 (Schrader and Yoon, 2007)	Mammalian	unknown	LLSM, BiFC, Confocal, STEDM	unknown
Mitochondria-LD	2011 (Wang et al., 2011)	Mammalian	contact regulation	EM, SR-FACT	Perilipin-5 (Wang et al., 2011)
Mitochondria-Vacuole (vCLAMP)	2014 (Honscher et al., 2014)	Yeast	survival in starvation and stress	EM, BiFC	TOM40-Vps39, Mcp1-Vps13 (Gonzalez Montoro et al., 2018) (vCLAMP)
Mitochondria-DB	2020 (Dong et al., 2020)	Mammalian	mitochondrial fission	SR-FACT	unknown
Golgi-Autophagosome	2015 (Biazik et al., 2015)	Mammalian	autophagosome formation	EM, ET	unknown
Lysosome-Peroxisome	2015 (Chu et al., 2015)	Mammalian	cholesterol transfer	FM, LLSM	Syt7 (Chu et al., 2015; Valm et al., 2017)
Lysosome-Autophagosome	1992 (Lawrence and Brown, 1992)	Mammalian	autophagosome formation	EM, ET, FM	Rab7-HOPS related complex (Jiang et al., 2014)
		Yeast	autophagosome formation	EM, ET, FM	Ypt7-HOPS related complex (Kirisako et al., 1999)
Lysosome-Endosome	1999 (Ohashi et al., 1999)	Mammalian	proper lysosomal digestive functions	EM, FM	Vamp8-Syntaxin 7 (Mullock et al., 2000),
		Yeast	endosome fusion regulation	FM	Rab7-HOPS-Rab7 (Nordmann et al., 2010; Balderhaar and Ungermann, 2013)
Lysosome-LD	2014 (Dugail, 2014)	Mammalian	lipid homeostasis	EM, FM, LLSM	PLIN2-HSC70-LAMP2A (Olzmann and Carvalho, 2019)
Lysosome-Golgi	2018 (Hao et al., 2018)	Mammalian	amino acid supply response	FM, PLA	mTORC1-Rheb (Hao et al., 2018)
Peroxisome-LD	2006 (Binns et al., 2006)	Mammalian	fatty acid trafficking	FIB-SEM, Confocal, LLSM, BiFC	M1 Spastin-ABCD1-ESCRT-III (Prinz et al., 2020)
		Yeast	fatty acid trafficking	FIB-SEM, Confocal, LLSM, BiFC	M1 Spastin-ABCD1-ESCRT-III (Prinz et al., 2020)
Peroxisome-PM	2018 (Kakimoto et al., 2018)	Yeast	unknown	BiFC	unknown
Peroxisome-Vacuole	2018 (Kakimoto et al., 2018)	Yeast	unknown	BiFC	unknown
Nucleus-Vacuole	1976 (Severs et al., 1976)	Yeast	microautophagy related	BiFC	Nvj1p-Vac8p (Kvam and Goldfarb, 2006), Lam6-Vac8 (Elbaz-Alon et al., 2015)
Nucleus-DB	2020 (Dong et al., 2020)	Mammalian	nuclear membrane formation	SR-FACT	unknown
LD-PM	2018 (Kakimoto et al., 2018)	Yeast	unknown	BiFC	unknown
LD-Vacuole	2018 (Kakimoto et al., 2018)	Yeast	unknown	BiFC	unknown
Vacuole-PM	2018 (Kakimoto et al., 2018)	Yeast	unknown	BiFC	unknown

The table summarizes MCSs and related information in different organisms. PM, plasma membrane; LD, lipid droplet; DB, Dark-vacuole body; vCLAMP, vacuolar and mitochondrial patch; ERMES, ER-mitochondria encounter structure; EM, electron microscopy; TEM, transmission electron microscope; Cryo-EM, cryogenic electron microscopy; ET, electron tomography; FIB-SEM, focused ion beam-scanning EM; FM, fluorescence microscope; Confocal, confocal microscopy; SIM, structured illumination microscopy; 3D-SIM, three-dimensional structured illumination microscopy; TIRFM, total internal reflection fluorescence microscopy; SR-FACT, super-resolution fluorescence-assisted diffraction computational tomography; LLSM, lattice light-sheet microscopy; STORM, stochastic optical reconstruction microscopy; STEDM, stimulated emission depletion microscopy; PLA, proximity ligation assay; FRET, fluorescence resonance energy transfer; BiFC, bimolecular fluorescence complementation; APEX, engineered peroxidase; APEX2, engineered variant of soybean ascorbate peroxidase.

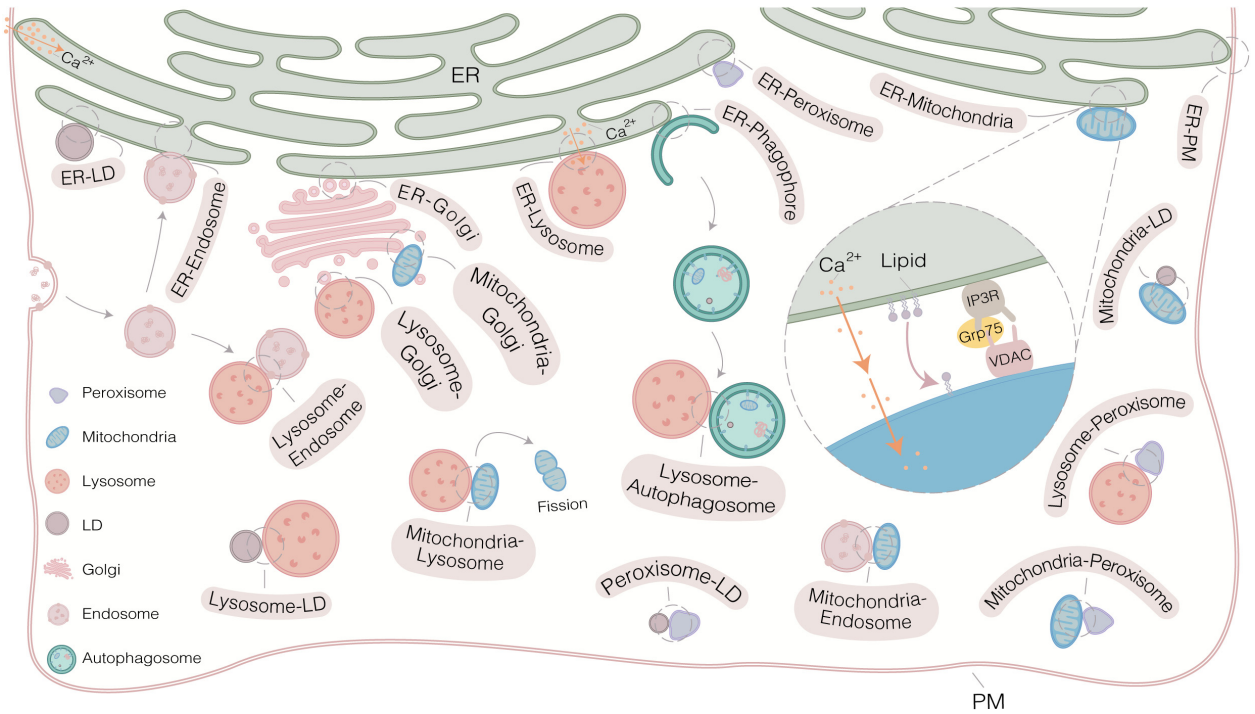

FIGURE 1 | Extensive membrane contact sites (MCSs) in mammalian cells. MCSs exist widely in cell and regulate exchanges signaling and regulates cellular functions. The common strategy for studying MCSs consists of various microscopies and biochemical approaches. Multiple canonical protein complexes have been reported to regulate MCSs, such as VDAC-IP3R-Grp 75 complex at ER-mitochondria MCS. Some MCSs, such as mitochondria-endosome MCS, Golgi-autophagosome MCS and lysosome-peroxisome MCS, are not shown due to limited space in this figure.

coupled with mass spectrometry (MS)-based proteomics, will facilitate the research of MCSs at the molecular and system level.

VISUALIZATION OF MCSs BY EM AND SRM

Electron microscopy provides the first evidence for ER-mitochondria MCS that improves the transfer of Ca^{2+} signal between both organelles in cells of the pseudobranch gland of a teleost (Copeland and Dalton, 1959; Rizzuto et al., 1998). Recently, EM and its variants, such as electron tomography (ET) and focused ion beam-scanning EM (FIB-SEM), are widely used to observe MCSs. High resolution structure of ER-mitochondria MCS was obtained by ET, an extension of traditional transmission EM (Csordas et al., 2006; de Brito and Scorrano, 2008). Two well-known structures, ER-mitochondria encounter structure (ERMES) and vacuolar and mitochondrial patch (vCLAMP) in yeast were directly observed by EM and ET (Kornmann et al., 2009; Honscher et al., 2014). The 3D ultrastructure of ER-PM MCS in COS-7 cells was visualized in close-to-native conditions by cryo-ET (Fernandez-Busnadiego et al., 2015; Fernandez-Busnadiego, 2016; Collado and Fernandez-Busnadiego, 2017). In FIB-SEM, a highly focused gallium ion beam ablates a thin layer of the sample after which the newly exposed surface is imaged with the scanning electron beam (Drobne, 2013; Fermie et al., 2018). FIB-SEM has recently been employed to systematically visualize ER MCSs with multiple other membranes including mitochondria and PM in neurons of mice (Wu et al., 2017). EM is regarded as the "gold standard" and exquisitely suited for investigation of MCSs, which provides fine architecture and spatial resolution of subcellular compartments. To some extent, EM has some drawbacks, such as fixation procedures, time-consuming and low through-put, restricting EM utility in living cells.

To enable visualization of MCSs in living cells, genetically encoded fluorescent proteins are tagged to resident proteins or tethers of different membranes so that MCSs become visible under multispectral fluorescence microscopy. Confocal microscopy is one of the most common methods to visualize subcellular localization of fluorescent membrane proteins. It has been employed to deconvolute and reconstruct 3D imaging of ER-mitochondria juxtaposition in living HeLa cells (Rizzuto et al., 1998) and of ERMES in yeast (Kornmann et al., 2009). To expand observation of dynamic multiple MCSs, lattice light-sheet microscopy (LLSM) was developed by using ultrathin light sheets from two-dimensional optical lattices (Chen et al., 2014). Multispectral imaging and computational analysis were introduced to visualize and quantify organelle interactome between six different organelles in COS-7 cells, such as ER, Golgi, lysosome, peroxisome, mitochondria and lipid droplet (LD) (Valm et al., 2017).

The dynamics and fine structure of MCSs require research tool with extreme high temporal and spatial resolution.

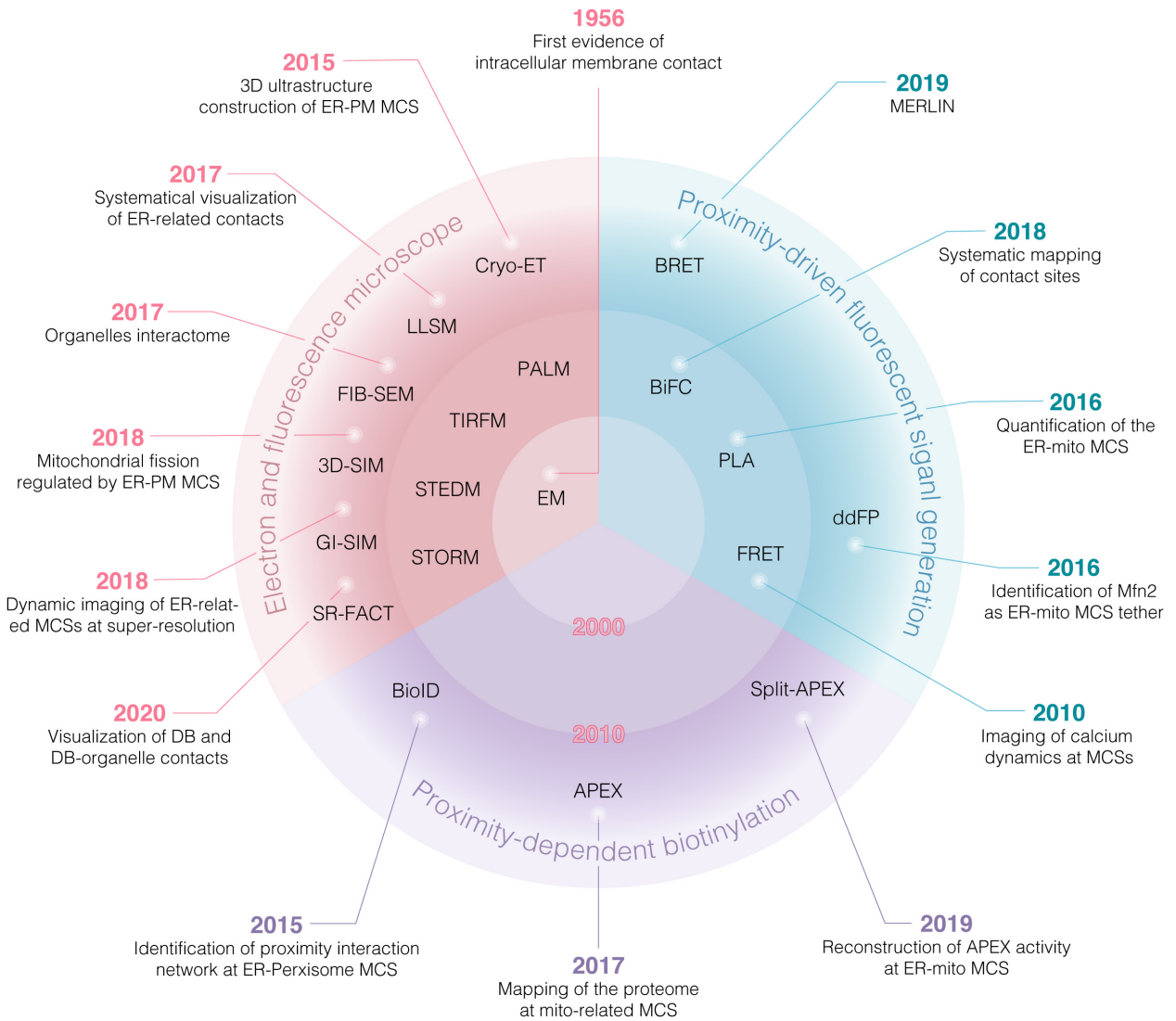

FIGURE 2 | Overview of various approaches for studying MCSs. Various approaches have greatly accelerated recent advances in MCSs at the system and molecular level. Before 2000, EM and confocal microscopy were most accessible tools. EM provided first evidence of intracellular membrane contact at nanoscale resolution, while confocal microscopy has been employed to reconstruct the 3D imaging of ER-mitochondria juxtaposition as sites of Ca^{2+} transfer between both organelles. Since 2010, super resolution microscopy (SRM) was increasingly used to visualize MCSs. Furthermore, proximity-driven fluorescent signal generation approaches, such as FRET, PLA, BiFC and ddFP were exploited to identify the potential MCSs. Notably, by combination with proteomic analysis, proximity-dependent biotinylation approaches mediated by BioID and APEX provide a promising strategy for global mapping MCSs and identification of tethers involving in MCSs, termed as "tether-omics." BRET, bioluminescence resonance energy transfer; BioID, proximity-dependent biotin identification; APEX, ascorbate peroxidase; MERLIN, mitochondria-ER length indicator nanosensor; FIB-SEM, focused ion beam-scanning EM; PALM, photoactivation localization microscopy; LLSM, lattice light-sheet microscopy; SR-FACT, super-resolution fluorescence-assisted diffraction computational tomography.

Super-resolution fluorescence microscopy (SRM) offers a unique window for the study of MCSs. Several SRMs, such as stimulated emission depletion microscopy (STEDM), photoactivation localization microscopy (PALM) and stochastic optical reconstruction microscopy (STORM), structured illumination microscopy (SIM), have been developed for imaging of nanoscale structural details and dynamics of MCSs, such as ER-PM MCS (Hsieh et al., 2017; Nascimbeni et al., 2017), ER-mitochondria MCS (Shim et al., 2012; Modi et al., 2019), ER-lysosome MCS (Shim et al., 2012), mitochondria-peroxisome MCS (Galiani et al., 2016). Among these SRMs, SIM is suitable for fast live-cell imaging and has been used to reveal numerous subcellular structures and dynamics (Li et al., 2015; Nixon-Abell et al., 2016; Zhanghao et al., 2019). Recently, ER-PM MCS in U2OS, Jurkat T and HEK293 cells was observed by SIM with total internal reflection fluorescence microscopy (TIRF-SIM) (Guo M. et al., 2018; Kang et al., 2019). The grazing incidence SIM (GI-SIM) was developed and applied to visualize ER-mitochondria, ER-late endosome and ER-lysosome MCSs in COS-7 and U2OS cells (Guo Y. et al., 2018). In addition, SIM based on Hessian matrixes

excels in extending the spatiotemporal resolution in live cells and is expected to apply for studying MCSs in COS-7 cells (Huang et al., 2018). More importantly, super-resolution fluorescence-assisted diffraction computational tomography (SR-FACT) was developed by combination of label-free three-dimensional optical diffraction tomography (ODT) with two-dimensional fluorescence Hessian structured illumination microscopy (Dong et al., 2020). The SR-FACT enable label-free visualization of various subcellular structures and complete division process of a COS-7 cell. By using SR-FACT, novel subcellular structures named dark-vacuole bodies (DB) were observed, and intensively contact with organelles such as mitochondria and nuclear membrane in COS-7 cells (Dong et al., 2020).

IDENTIFICATION OF MCSs BY PROXIMITY-DRIVEN FLUORESCENT SIGNAL GENERATION

Confocal microscopy is used to visualize subcellular localization of fluorescent membrane proteins, rather than suitable to study MCSs. On one hand, co-localization of resident proteins or tethers of different membranes observed by confocal microscopy, however, doesn't mean the existence of MCS. On the other hand, because of continuing organelles movement, dynamic MCSs are difficult to detect by confocal microscopy alone with low resolution. The proximity-driven fluorescent signal generation enable identification of MCSs with more reliability and easy operation. Briefly, two fragments or proteins fused with organelle markers or tethers, reside on outer membrane of different organelles, are each no signal or low signal on their own but are reconstituted to give strong fluorescent signal when driven together by membrane proximity. These approaches are widely used to visualize MCSs and identify important tethers involving in MCSs (**Figure 3** and **Table 1**).

PLA

Proximity ligation assay (PLA) is a unique method for protein detection. In PLA, single-stranded oligonucleotides are conjugated to affinity binders or antibody of proteins, followed by amplification of the signal by rolling-circle amplification (RCA) and detection of complementary fluorophore labeled oligonucleotides (Fredriksson et al., 2002; Schallmeiner et al., 2007; Soderberg et al., 2008). PLA has success to observe interaction of individual endogenous protein complexes *in situ* (Soderberg et al., 2006; Fredriksson et al., 2007), which validates protein-protein interactions in multiplexed proteins.

Recently, PLA has been employed to address MCSs. Dual binding by a pair of proximity probes (antibodies with attached DNA strands) to two membrane resident proteins or tethers serves to template the hybridization of circularization oligonucleotides, which is then joined by ligation into a circular DNA molecule (**Figure 3A**). ER-mitochondria MCS was visualized and quantified by using the close proximity between voltage-dependent anion channel 1 (VDAC1, localizes in outer mitochondrial membrane) and inositol 1,4,5-triphosphate receptor (IP3R, localizes in ER membrane) at the mitochondria-associated membranes (MAMs) interface in human HuH7 cells (Tubbs and Rieusset, 2016). The VDAC1-IP3R PLA system was used to reveal the role of ER-mitochondria tethering complex VAPB-PTPIP51 in regulating autophagy in HeLa and HEK293 cells (Gomez-Suaga et al., 2017). In addition, by using VDAC1-IP3R PLA system, Stoica et al. found that ALS/FTD-associated FUS activates GSK-3β to disrupt the VAPB-PTPIP51 interaction and ER-mitochondria associations in NSC-34 mouse motor neuron cells (Stoica et al., 2016), and Thomas et al. revealed that phenformin blocks MAMs that support autophagy in HEK293 cells (Thomas et al., 2018). ER-lysosome MCS was detected by PLA, and further experiment confirmed that the clusters of IP3R populate ER-lysosome MCS and facilitate local delivery of Ca^{2+} from the ER to lysosome (Atakpa et al., 2018).

FRET

Fluorescence resonance energy transfer is one of most accessible technologies that allow for detecting protein-protein interaction at super resolution. FRET was primally from Förster's theory, in which dipole-dipole interaction made the photon energy transfer from excited donor to acceptor between an energy donor-acceptor fluorescent pair when the distance between donor and acceptor was 1 to 10 nm. FRET is a non-destructive method of spectroscopy and therefore applied to observe the signal of MCSs in living cells (Zimmer, 2002; Pietraszewska-Bogiel and Gadella, 2011; Marx, 2017; **Figure 3B**). Fluorescent proteins were derived from 1980s when green fluorescent protein (GFP) of *Aequorea victoria* was exploited as a GFP-chimera targeted to specific organelles membrane and further optimized to the mutants, such as RFP and BFP (Rizzuto et al., 1996; Zimmer, 2002). Normally, fluorescent proteins fused with membrane proteins or tethers are used as donor/acceptor probes. The combination between fluorescent proteins and FRET brings a great progress for the great integration with targeted protein. FRET has been exploited to be a useful tool by combination with other technologies. Combination between fluorescence lifetime imaging (FLIM) and FRET offers direct evidence of temporal membrane proximity at high resolution (Bastiaens and Squire, 1999; Elangovan et al., 2002; Sekar and Periasamy, 2003). Photoswitching FRET (psFRET), a revised version of photobleaching FRET (pb FRET) of which detection of fluorescence signal required only imaging of donor before and after photobleaching of acceptor (Wouters et al., 1998). Improvement of psFRET make photobleach to be switched "off" and be re-detectable (Rainey and Patterson, 2019). Recent work systematically assessed the FRET from principle to screening of donor-acceptor pair (Algar et al., 2019).

Fluorescence resonance energy transfer is an indispensable experimental tool for the study of the MCSs (Jing et al., 2015; Subedi et al., 2018). Tandem GFP pairs allowed for detecting the alteration of intracellular Ca^{2+} level at mitochondria-ER MCS in HeLa and HEK293 cells, in which tandem expression of BFP-CBD (26-residue containing calmodulin-binding domain)-EGFP was sensitive to change of Ca^{2+} flux that causes a structural alteration of CBD and a destroyed FRET pair (Miyawaki et al., 1997; Romoser et al., 1997). Cooperation between FRET and total internal reflection microscopy (TIRFM) was designed to study

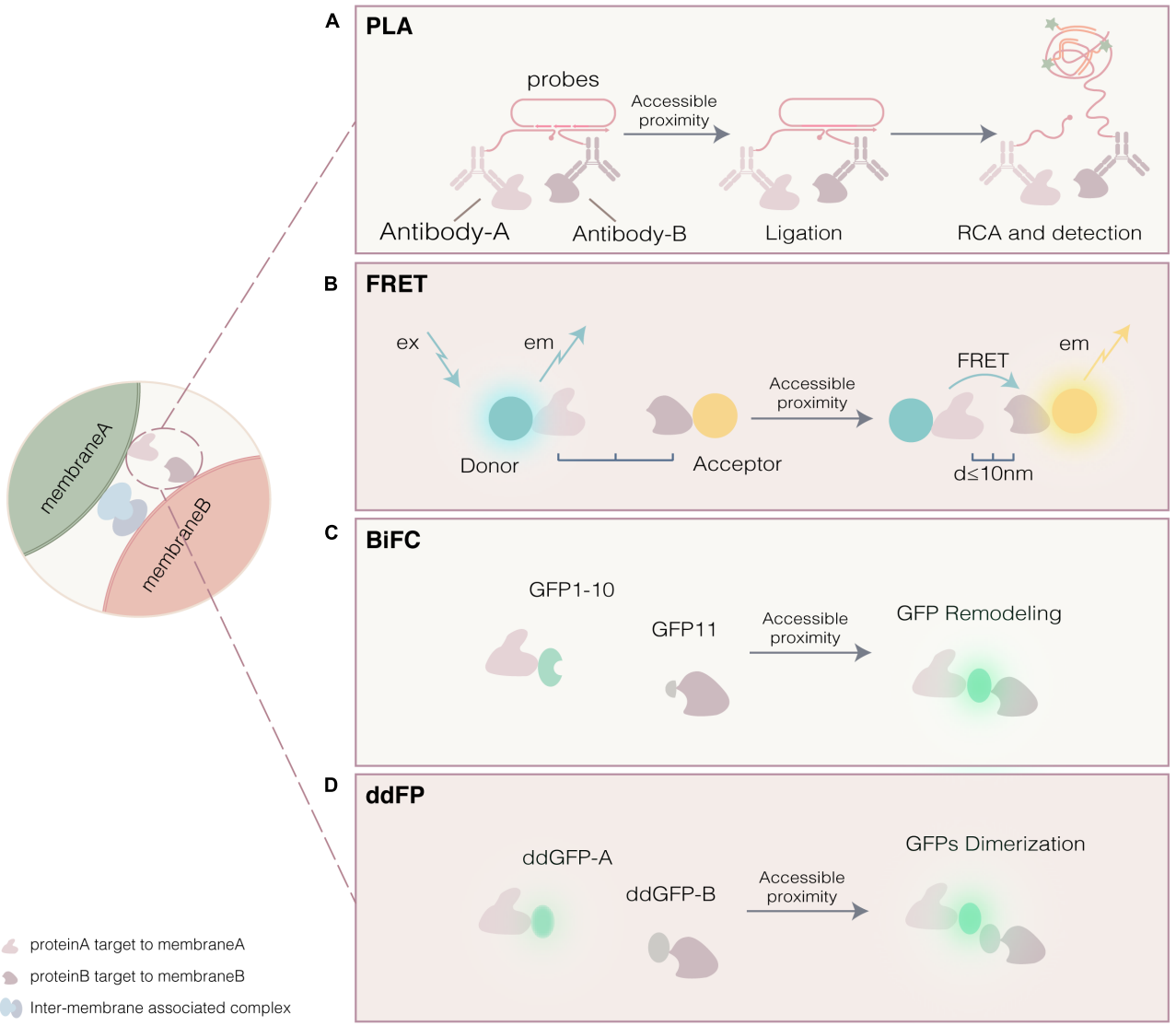

FIGURE 3 | Proximity-driven fluorescent signal generation approaches. **(A)** Proximity ligation assay (PLA). Single-stranded oligonucleotides are conjugated to antibody of proteins. Membrane proximity serves to template the hybridization of circularization oligonucleotides, which is then joined by ligation into a circular DNA molecule and followed by amplification of the signal by rolling-circle amplification (RCA). **(B)** Fluorescence resonance energy transfer (FRET). The photon energy transfers from excited donor to acceptor since the accessible proximity. **(C)** Bimolecular fluorescence complementation (BiFC). Accessible proximity made GFP1-10 and GFP11 remodel into a mature fluorescent protein. **(D)** Dimerization-dependent fluorescent proteins (ddFP). Two GFP monomer (ddGFP-A and ddGFP-B) with weak signal form a dimer with fluorescent strong signal since the accessible proximity.

ER-PM MCS in RBL-2H3 (mice) and HeLa cells (Poteser et al., 2016; Chen et al., 2017; Chang et al., 2018). FRET was applied to study lipid transfer regulated by oxysterol-binding protein (OSBP) at the MCSs between ER and other organelles in human RPE1 cells (Jamecna et al., 2019). Furthermore, another improved method is that FK506-binding protein 12 (FKBP 12) and FKBP 12-rapamycin binding domain (FRB) were anchored to different organelles by each resident membrane protein, respectively. As rapamycin induction, the closely spatial FKBP and FRB interact with each other, which activates FRET signal (Inoue et al., 2005). This method was applied to study ER-mitochondria MCS in rat H9C2 cardiomyoblast cells and basophilic leukemia (RBL)-2H3 cells (Csordas et al., 2010) and identify ER-mitochondria MCS tether Mfn2 in MEF cells (Naon et al., 2016). In another study, FRET venus-mTurquoise2 pair was fused to TOM20 and LAMP1 respectively, to study the regulation of mitochondria-lysosome MCS mediated by mitochondria fission via Rab7 GTP hydrolysis in HeLa cells (Wong et al., 2018).

A variant of FRET technique, bioluminescence resonance energy transfer (BRET) has been developed to study protein-protein interactions (Pfleger and Eidne, 2006). In BRET, the donor is luciferase enzyme which catalyzes a bioluminescent oxidation, and then the energy is transferred to the acceptor by resonance if the protein-protein interacts occurs. Compare with

FRET, BRET does not require sample illumination to excite the donor and has been emerged as a powerful tool for the study of protein-protein interactions (Perroy et al., 2004; De, 2011; Mo and Fu, 2016). Recently, a novel BRET-based biosensor with Renilla Luciferase 8 (RLuc) acting as a donor and mVenus as an acceptor, named MERLIN (mitochondria-ER length indicator nanosensor), was presented for the analysis of distances between ER and mitochondria in COS1 and HCT116 cells (Hertlein et al., 2020). In MERLIN, mVenus was targeted to mitochondria by the alpha-helical C-terminal domain of Bcl-xL (B33C) and RLuc was targeted to ER by a truncated non-functional variant of calnexin (sCal). The further experiments have demonstrated that MERLIN is a powerful and innovative tool for the investigation of ER-mitochondria MCS.

Bimolecular Fluorescence Complementation

Bimolecular complementation (BiC) system was successful applied in multiple proteins, such as ubiquitin (Johnsson and Varshavsky, 1994), β-lactamase (Galarneau et al., 2002), firefly (Luker et al., 2004) and fluorescent proteins. Bimolecular fluorescence complementation has emerged as a key technique to visualize protein-protein interactions in living cells. In BiFC system, split-fluorescent protein composes of two complementary protein residues, each no fluorescent signal on their own but are reassemble to give the bright fluorescence when driven together by protein interaction. In the earlier split-GFP system, GFP protein was divided into GFP-N (residues 1–157) and GFP-C (residues 158–230) with fused to leucine zipper, respectively. Leucine zipper interaction drive refold of GFP protein and the green fluorescence was recovered (Magliery et al., 2005). Because of low efficiency of fluorescence recovery, a more effective system, split super-folder GFP was engineered for efficient self-complementation without leucine zipper or other protein-protein interaction (Cabantous et al., 2005). In this method, GFP protein was divided into GFP1-10 (residues 1–214) fragment and GFP11 (residues 214–230) fragment, of which GFP 1-10 fragment contains three residues of the fluorophore. Only if GFP1-10 complement with the conserved residue E222 at GFP11, the fluorophore is reactive with brightest green fluorescence (Cabantous et al., 2005). For successful construction of split-fluorescent system, each individual protein residue cannot show any protein activity, and each individual protein residue cannot show a distinct fluorescent activity, instead a strong signal should be detected when reassembled (Magliery et al., 2005; Shekhawat and Ghosh, 2011). Notably, engineered GFP mutants were always considered due to the limited GFP fluorescent intensity (EGFP and Venus) (Wiens and Campbell, 2018). For the signal irreversibility, this method was commonly competent to detect transient protein-protein interaction (Magliery et al., 2005), instead of temporal information of protein-protein interaction.

Bimolecular fluorescence complementation is able to sensitively detect MCSs, where the contact signal always shows stable dots (**Figure 3C**). ER membrane protein Ifa38 and mitochondrial outer membrane protein TOM71 fused to GFP 1-10 and GFP11, respectively, highlight the signal of ER-mitochondria MCS as dots in yeast and HeLa cell. LD-peroxisome MCS can also be labeled with this split system mediated by LD protein Erg6 and peroxisome protein Pex3 in yeast (Kakimoto et al., 2018). The GFP variants, such as Venus, mCherry, and FusionRed, were also exploited to study MCSs (Toulmay and Prinz, 2012; Lahiri et al., 2014; Wiens and Campbell, 2018). Venus protein was derived from GFP and carries five amino acids mutation with improved brightness (Rekas et al., 2002). Similar with split GFP, split-Venus was developed and applied to detect MCSs such as ERMES, ER-LD MCS and vCLAMP in yeast (Shai et al., 2018). More importantly, split-Venus was employed to uncover new MCSs in yeast, such as vCOuPLE (vacuole-plasma membrane contact), pCLIP (plasma membrane-lipid droplet), PerPECs (peroxisome-plasma membrane) and PerVale (peroxisome-vacuole) (Shai et al., 2018). The split-Venus also was used to detect ER-mitochondria junctions, further experiment has demonstrated that ER membrane protein complex (EMC) tethers ER to mitochondria, which is required for phospholipid synthesis and cell growth in yeast (Lahiri et al., 2014). BiFC was employed to detect plastic remodeling of ER-mitochondria MCS and it is demonstrated that ER-mitochondria MCS is dynamic structure that undergoes active remodeling under different cellular needs in human osteosarcoma U2OS cells (Yang et al., 2018).

Recently, to expand BiFC toolset, direct engineering of self-complementing split fluorescent protein was developed by insertion a 32 amino acid spacer between the tenth and eleventh β-strands of GFP. The dual-color endogenous protein was tagged with sfCherry2 11 and GFP 11, revealing that the abundance of ER translocon complex Sec61B reduced in certain peripheral tubules. The new BiFC system offers multiple colors for imaging MCSs in HEK293T cells (Feng et al., 2017). In addition, a split GFP-based contact site sensor (SPLICS) was designed to detect the wide or narrow membrane contacts (narrow: 8–10 nm and wide: 40–50 nm) by the flexible spacer linked between GFP11 and ER targeting sequence. The ER-mitochondria MCS was allowed for detection and monitored by using this sensor in HeLa and HEK293 cells (Cieri et al., 2018).

ddFP

Dimerization-dependent fluorescent protein (ddFP) is a class of genetically encoded reporters based on the reversible binding of two dark fluorescent protein monomers to form a fluorescent heterodimeric complex, which can be used for detection of protein-protein interactions in living cells (Ding et al., 2015; Mitchell et al., 2018). The yellow or red fluorescent proteins are obligate tetrameric, however, is limited by its tetramerization disruption. To solve this problem, multiple monomeric fluorescence proteins were obtained through amino acid mutation, such as dTomato, mCherry and mStrawberry (Shaner et al., 2004). These monomeric proteins act as basic components to employ the ddFP tool. For earliest version of ddFP construction, a monomeric fluorescent dTomato variant (H162K and A164R) and a suitable "aptamer" (engineered another dTomato monomer) were screened. The "aptamer" allowed to constitute a heterodimer with the dTomato variant. Both two engineered dTomato monomer exhibited a weak red

fluorescence, however, the spatial proximity induced formation of the heterodimer through non-covalent interaction to exhibit a brighter fluorescent signal (Alford et al., 2012a). Furthermore, ddGFP was engineered with brighter fluorescent signal exhibited ∼60-fold increase in emission intensity upon heterodimerization. The protein-protein interaction can act as an indicator when two monomers are spatial proximity and thus an ideal tool for the study of MCSs. The advantage of ddFP is its reversibility, which is suitable to measure the dynamics of MCSs (**Figure 3D**).

By using ddGFP tool, a highly effective indicator of membrane proximity was generated to image MAM interface of ER and mitochondria by fusing two monomers of fluorescent protein to endoplasmic reticulum membrane (ERM) and outer mitochondrial membrane (OMM), respectively in HeLa cells (Alford et al., 2012b). When their spatial distance was less than 20 nm, a heterodimer was reconstructed by non-covalent interaction between monomers and then produce a stronger fluorescent signal. The ddGFP signal at ER-mitochondria MCS reduced when Mfn2, a crucial ER-mitochondria MCS tether, was deleted in MEF cells (Naon et al., 2016). The mutant TDP-43 did not impair mitochondrial bioenergetics by using ddGFP targeted to mitochondria and ER (TOM20-ddGFP and calN-ddGFP, respectively) in HeLa cells (Kawamata et al., 2017).

GLOBAL MAPPING MCSs BY PROXIMITY-DEPENDENT BIOTINYLATION

Inter-organelle membrane contact sites are established and maintained by tethers (**Table 1**). Although MCSs have been widely observed by EM and fluorescence techniques, tethers remained to be explored. Almost identified MCSs are mediated by multiple tethering proteins or protein complex, rather than only one tether. Some tethers were identified to mediate MCSs by traditional biochemical approaches, such as cell fractionation and pull-down. However, several considerable defects limit their application. Firstly, these approaches fail to catch the transient membrane contact; Secondly, the MCSs might be destroyed when detergent is added; Lastly, the dynamics of MCSs can't be monitored. The proximity biotinylation approaches such as proximity-based biotin identification (BioID) and ascorbate peroxidase (APEX) tagging are used to label neighboring proteins by generating a reactive biotin derivative (**Figure 4**). These proximity-dependent biotinylation approaches combined with proteomic analysis provide a promising strategy for global mapping MCSs.

BioID

Proximity-based biotin identification technology is dependent on BirA, a 35 kD DNA-binding biotin protein ligase that regulates the biotinylation of a subunit of acetyl-CoA carboxylase and inhibits biotin biosynthetic operon (Lane et al., 1964). For biotinylation, native biotin binds with ATP to constitute a biotinoyl-5′-AMP (BioAMP) prior to target to active site of BirA, biotin is then ligated to lysine residue when BAT sequence, a biotin acceptor tag, is recognized by BirA. Compared with BirA, BirA* (a R118G BirA mutant) with a lower affinity toward BioAMP causes promiscuous protein biotinylation. BioID enables to biotinylate potential proteins in proximity-dependent manner (Cronan, 2005; Gupta et al., 2015; Gingras et al., 2019). Cells expressing a bait resident protein fused to BirA* tag are incubated with biotin for several hours and then the biotinylated proteins are captured on a streptavidin affinity matrix for identification by LC-MS/MS (**Figures 4A,B**). BioID technology has proven to be a powerful method for identifying proximal proteins in cells.

The tethers involving in ER-peroxisome MCS were identified by BioID (Hua et al., 2017). PEX16 a key peroxisomal biogenesis protein and initially targets to the ER before the traffic to peroxisomes in COS-7 cells (Hua et al., 2015). By using BioID, a proximity interaction network (70 high-confidence proximal interactors) for PEX16 was mapped in human 293 T-REx Flp-In cells. The further experiment highlighted that ER-resident VAMP-associated proteins A and B (VAPA and VAPB) interact with peroxisomal membrane protein acyl-CoA binding domain containing 5 (ACBD5), which is required to tether two organelles together and thereby facilitates lipid exchange between the organelles in COS-7 cells. BioID was also used to investigate the role of tethers in ER-PM MCS. Unfolded protein response (UPR) PERK-BirA proximity interactome was obtained, and furthermore, actin-binding protein filamin A (FLNA) was identified as a key PERK interactor. The work revealed the role of PERK as a multimodal organizer of MCSs between ER and other vital organelles. As an apical sensor of ER-Ca^{2+} store alterations, PERK was able to tightly couple store depletion to facilitate the expansion of ER-PM MCS through interaction with FLNA and spatial organization of actin cytoskeleton in HEK293T cells (van Vliet et al., 2017).

In addition, as its effectiveness, split-BioID was exploited to uncover the PP1-interacting proteins (PIPs) targeted by protein phosphatase PP1 in HEK293T cells (De Munter et al., 2017). In split-BioID, BirA* was divided into BirA*-N and BirA*-C (at amino acid 140/141). The enzyme activity of BirA* is reconstructive after heterodimerization of BirA*-N and BirA*-C fragments.

APEX

Ascorbate peroxidase is an engineered ascorbate peroxidase. In the presence of hydrogen peroxide, APEX not only catalyzes 3,3′-diaminobenzidine (DAB) to generate an electron-dense product for visualization by EM (**Figure 4C**; Martell et al., 2012), but also converts a phenolic substrate (biotin-phenol) into a highly reactive radical and covalently tags proximal endogenous proteins (Rhee et al., 2013; Hung et al., 2014). Because the limited sensitivity of APEX precludes applications requiring low APEX expression, more active form APEX2 for intracellular specific protein imaging by EM and spatially-resolved proteomic mapping was obtained by yeast display evolution (Lam et al., 2015). In the presence of the APEX2 substrate biotin-phenol, a brief pulse of hydrogen peroxide (H_2O_2, < 1 min) results in the APEX2-catalyzed generation of short-lived, membrane impermeable biotin-phenoxyl radicals that form covalent adducts

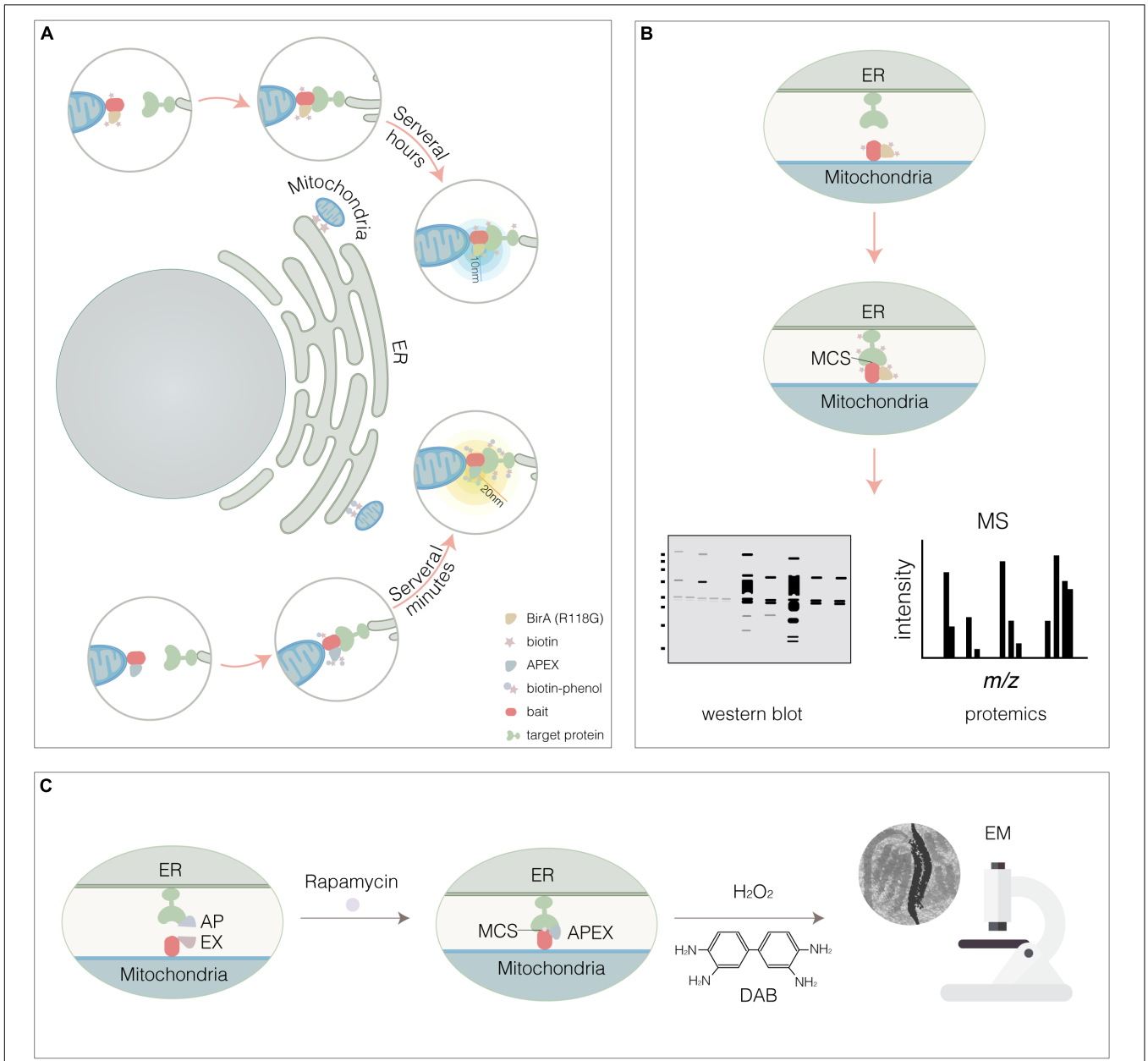

FIGURE 4 | Proximity-dependent biotinylation approaches. **(A)** BioID- or APEX-based proximity labeling. BirA* (Upper panel) or APEX (Lower panel) were fused to mitochondria membrane protein (bait). The potential target that be thought to interact with bait within the accessible proximity (10 nm for BirA*, 20 nm for APEX) would be biotinylated. For BirA*, endogenous biotin was accessible, instead APEX required the exogenous biotin-phenol and H_2O_2. **(B)** Cell expressing BirA*-bait or APEX-bait were lysed, then the biotinylated targets were captured by streptavidin-beads and identified by WESTERN BLOT and MS. **(C)** Reconstitution of split-APEX at ER- mitochondria MCS. By AP fused to $TOM20^{1-34}$ for targeting OMM and EX fused to $Cb5^{100-134}$ for targeting ERM, respectively, the split APEX enzyme activity was reconstituted and ER-mitochondria MCS was visualized at higher resolution by EM through the combination of the DAB staining.

with electron-rich amino acids in proteins located within a 10–20 nm radius, which enables to mark the potential proteins involving in MCSs (**Figures 4A,B**).

Ascorbate peroxidase has been successfully applied to localize mitochondria at proteomic level without mitochondria purification (Rhee et al., 2013), and also give insights into the composition and dynamics of LD proteomes in human osteosarcoma U2OS cells (Bersuker et al., 2018). The proteome at ER-mitochondria MCS was mapped by using APEX. The tethers localizing at the MCS between mitochondria and other organelles were identified and validated by combining biochemical subcellular fractionation. For instance, atlastin (ATL2) and reticulon (RTN1 and RTN3) are critical in forming ER-mitochondria MCS in HEK293 cells (Cho et al., 2017). Another work focused on ER-mitochondria MCS using APEX2 (Hung et al., 2017). By using APEX2-mediated proximity

biotinylation, endogenous proteins on the OMM and ERM of living human fibroblasts were captured and identified. By mining OMM and ERM proteomic data, it is reported that the tail-anchored OMM protein synaptojanin-2 binding protein SYNJ2BP was observed richly in both OMM- and ERM-targeted APEX2. The overexpression of SYNJ2BP dramatically increases ER-mitochondria MCSs mediated by RRBP1, SYNJ2BP's binding partner on the ER membrane.

To further advance the capabilities of APEX in protein-protein interactions and MCSs, split APEX2 was engineered. APEX2 was divided into N- and C-terminal fragments (at amino acid 201/202) for protein complementation assays (Xue et al., 2017). In addition, split APEX2 tool with more efficiency was engineered using directed evolution (Han et al., 2019). A total of 20 rounds of fluorescence activated cell sorting (FACS)-based selections from yeast displayed fragment libraries produced a 200-amino-acid N-terminal fragment (with 9 mutations relative to APEX2) called "AP" and a 50-amino-acid C-terminal fragment called "EX." AP and EX fragments were each inactive on their own but were reconstituted to give peroxidase activity when driven together by MCS. By AP fused to $TOM20^{1-34}$ for targeting OMM and EX fused to $Cb5^{100-134}$ for targeting ERM, respectively, the split APEX enzyme activity was reconstituted and ER-mitochondria MCS was visualized at higher resolution by EM through the combination of the DAB staining in HEK293T cells (**Figure 4C**; Han et al., 2019). Expectably, split-BioID and split APEX technologies that combine reporter-fragment complementation and proximity-dependent biotinylation will be promising tools to map MCSs and identify new tethers.

CONSIDERATIONS OF VARIOUS APPROACHES FOR STUDYING MCSs

In living cells, individual organelles are highly dynamic, so MCSs show a highly dynamic spatiotemporal pattern to response to various external stimuli. For example, ER enable enlarge its cytoplasmic volume from ∼35 to 97%, and mitochondria from ∼10 to 70% in 15 min in COS-7 cells (Valm et al., 2017), which drives transient alteration of MCSs. As described in previous chapters, although several different types of microscopies and various biochemical techniques are available for the study of MCSs, their principal drawbacks should be considered to avoid to gain the false positive or false negative results.

For the electron and light microscopy, spatiotemporal resolution and imaging condition have been supposed to be crucial for the study of MCSs. EM, FIB-SEM, and cyro-ET of cell specimen at the nanometer scale enable observation of subcellular structures of MCSs without fluorescence labeling. Although EM and FIB-SEM provide the fine structure details of MCSs with extreme spatial resolution, the fixation and dehydration procedures of EM tend to disrupt the intact architecture of intracellular organelles and MCSs. Cyro-ET allows thin samples to be imaged in 3D in a nearly native state by immobilizing samples in non-crystalline ice without fixation and dehydration procedures. However, like EM and FIB-SEM, cyro-ET is impossible to detect the dynamics of MCSs in living cells (**Figure 5A**). Light microscopy based on fluorescence was developed in living cells to overcome fixation procedures and low through-put of EM. Confocal microscopy is one of the most common methods to visualize the subcellular localization of fluorescent membrane resident proteins, however, confocal microscopy alone is not good choice to detect membrane contacts because of low spatiotemporal resolution. The combination of confocal microscopy and biochemical techniques (proximity-driven fluorescent signal generation) confers to powerful approaches for the study of MCSs. Super-resolution fluorescence microscopy (SRM), such as STEDM, PALM, STORM, and SIM, offers a unique window with super temporal and spatial resolution in living cells for MCSs. Especially, GI-SIM show extremely great advantage in the study of MCSs dynamics because of the extreme high temporal and spatial resolution. Compare to EM, fluorescence labeling of organelles is requisite to light microscopy. In addition, SRM imaging are mostly available in imaging facilities and a small number of laboratories due to its high cost, even some of them are not commercial (**Figure 5A**).

The reversible biochemical tools are required to catch the dynamics of MCSs. PLA is able to detect protein-protein interactions on endogenous levels and does not require a superior quantity of protein in comparison to traditional fluorescent fusion protein expression. More importantly, the quantitative analysis of MCSs can be accessed by PLA. However, some antibodies for endogenous proteins are not available. The fixation step is also necessary for PLA, which renders PLA to monitor the dynamic MCSs. FRET between donor- and acceptor-tagged membrane proteins is a quite suitable tool for dynamics of MCSs because FRET is dependent on non-interacted and distance-dependent fluorescence excitation. The optimization of FRET sensor and special microscopy set-up, however, are required. Notably, the equivalent expression of donor and acceptor are required in cell for the study of MCSs. BiFC gives the bright fluorescence when driven together by inter-organelle membrane proximity and is a widely used biochemical tool for the study of MCSs. BiFC allows to detect the transient organelles contact. The drawbacks of BiFC should be carefully considered. Irreversible binding of split FP fragments leads to accumulation of the fluorescent signal and stabilizes the MCSs, which could cause false-positive signals (Eisenberg-Bord et al., 2016). In brief, based on reversible dimerization, ddFP is a highly effective indicator of inter-organelle membrane proximity. In ddFP, low-fluorescence intensity of the probes could restrict its application. Except for PLA, the approaches based on proximity-driven fluorescent signal generation enable identification of MCSs in high confidence and high dynamic state in living cells. Therefore, the above biochemical techniques are widely used to study MCSs and their principal drawbacks should be considered (**Figure 5B**).

The proximity-dependent biotinylation approaches have been supposed to a promising tool to identify new tethers involving in MCSs. Because of dynamics of MCSs, labeling time is a crucial parameter when the proximity-dependent biotinylation approaches are employed to study MCSs in living cells. Generally, 12–24 h was required for biotinylation by BioID, and it take at least 3 h to finish labeling (Youn et al., 2018; Gingras et al., 2019). Instead, the biotinylation based on APEX2 required ∼30 min

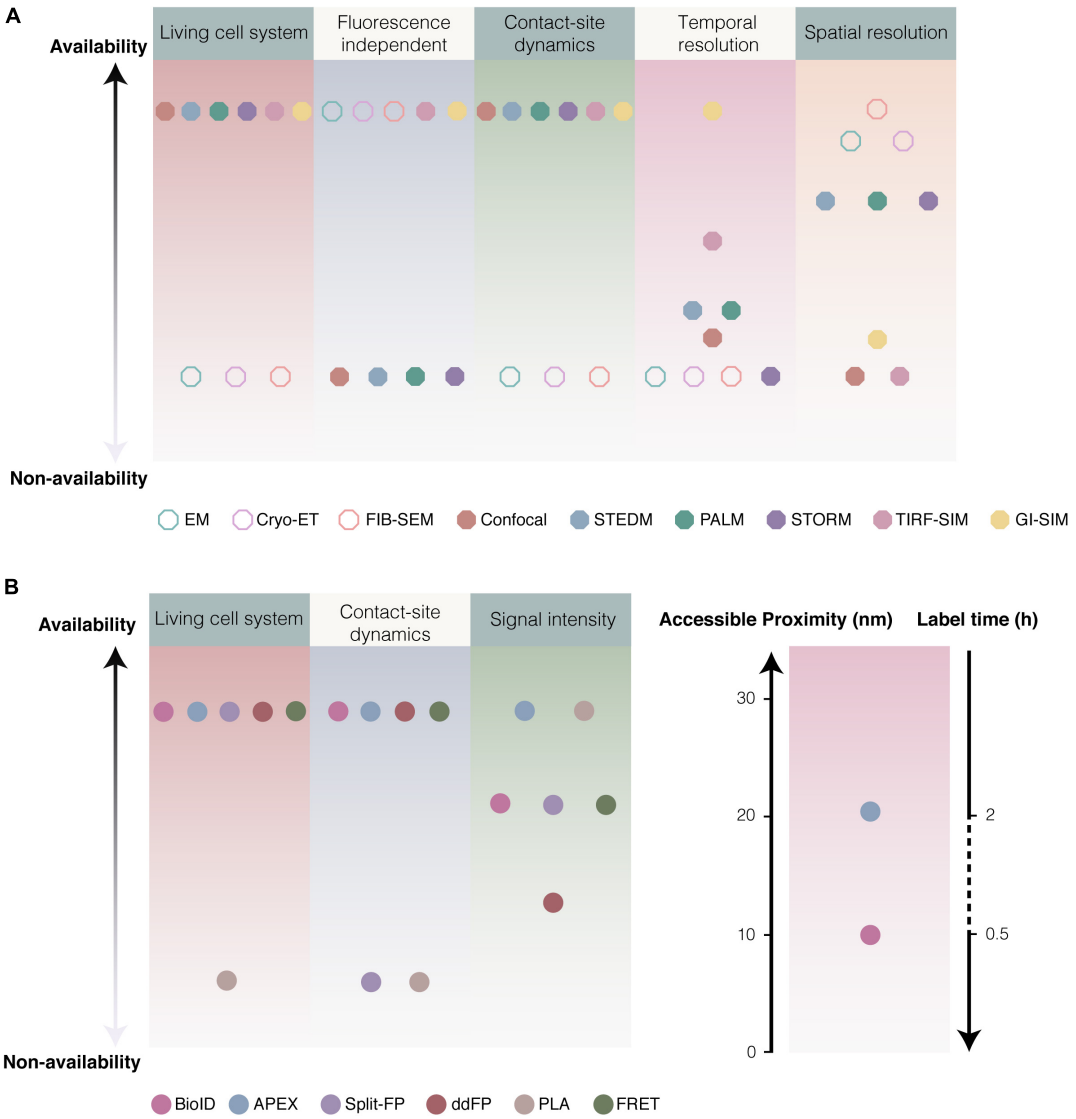

FIGURE 5 | Considerations of various approaches for studying MCSs. **(A)** Comparison of various microscopies. Imaging of EM, Cryo-ET and FIB-SEM are fluorescence independent with high resolution (1.8–4 nm), rather than suitable for the dynamics of MCSs in living cell. Comparison to confocal (<0.5 Hz, ∼200 nm) (Schulz et al., 2013), super resolution fluorescence microscopy like STEDM (Schneider et al., 2015), PALM (Betzig et al., 2006; Gould et al., 2009) and STORM (<10 Hz, ∼20 nm) (Rust et al., 2006), GI-SIM (266 Hz and 97 nm) (Guo Y. et al., 2018) as well as combination TIRF with SIM (TIRF-SIM: ∼11 Hz, 100 nm) (Kner et al., 2009) showed extreme high temporal and spatial resolution. **(B)** The availability of various biochemical techniques. Generally, 12–24 h was required for biotinylation by BioID, while biotinylation based on APEX2 required ∼30 min. BirA* enable to effectively label proteins at distance ∼10 nm, and APEX at ∼20 nm.

only, that is an obvious advantage of APEX2 compared with BioID (**Figure 5B**). In addition, BirA* is able to biotinylate the potential proteins using exogenous biotin as well as endogenous biotin. Whereas, APEX2 catalyzes the substrate biotin-phenol that is only from external supplement. If BirA* is anchored to membrane contact by transfection the fusion construct, it is possible to capture false positive proteins because of long labeling time and utilization of endogenous biotin. A new technology called TurboID or miniTurbo was reported to finish biotinylation in 10 min in HEK293 cells (Branon et al., 2018; Mair et al., 2019).

Inter-organelle membrane contact sites allow subdomains of organelle membranes to contact within 10–50 nm, in which membranes were considered to be spatial proximity and even exist lipids and signal (Ca^{2+}) transfer. For the biochemical techniques, it should be considered whether the distance reached by tools is suitable for the spatial proximity between inter-organelle membranes. PLA might lengthen its effective distance up to 30 nm (even more wider) as the adjustable length of nucleic acid arms and antibody affinity, which cause more false positive signals. FRET is able to detect a narrow contact with a typical range of roughly 1–10 nm (and up to 10 nm for atypical FRET pairs). Recently, split-GFP-based contact site sensor (SPLICS) was engineered to measure narrow (8–10 nm) and

wide (40–50 nm) juxtapositions between ER and mitochondria by increasing the length of the spacer of the probe and resident protein. In addition, labeling radius of BioID/APEX should be considered, BirA* enable to effectively label proteins at distance ∼10 nm (Kim et al., 2014), and APEX labeling ∼20 nm (Gingras et al., 2019). Therefore, the linker length between probe/enzyme and resident protein should be seriously considered when the proximity-driven fluorescent signal generation and proximity-dependent biotinylation are employed to study MCSs.

Given the diameter of general subcellular apparatus, BioID and APEX enable to ensure the signal reliability to uncover potential tethers (**Figure 3B**). However, some tethers involving in wide contacts could be missed because labeling radius of BioID/APEX does not reach the distance between the enzyme and candidate tethers. If the linker length between bait and BirA*/APEX is too long, it is easy to lead lots of false positives. To overcome this drawback, multiple baits or split-BirA*/APEX could be used to map MCSs. The remodeling of AP and EX in split-APEX be thought to maintain normal MCSs (Han et al., 2019). Instead, EGFP fusion overexpression always cause abnormal membrane contact (Snapp et al., 2003; Hung et al., 2017).

Overall, the drawbacks and limitations should be considered to keep in mind when these approaches are used to the study of the dynamic MCSs.

CONCLUSION AND PERSPECTIVES

The various microscopies, proximity-driven fluorescent signal generation and proximity-dependent biotinylation have greatly accelerated the recent advances of MCSs at the molecular and system level. The drawbacks of various approaches should be considered to keep in mind when these approaches are used for the study of dynamic MCSs. To overcome the limitations, the approaches combination would be a better choice for the study of MCSs.

In the near future, full scenario of MCSs will be presented using the current and emerging approaches. On one hand, the high temporal-spatial resolution microscopies will be used to draw the extensive MCSs (organelles interactome). On the other hand, biochemical techniques, especially proximity-driven biotinylation coupled with MS-based proteomics will be sharpest tools to map MCSs and identify new tethers involving in MCSs, termed as "tether-omics." In addition, cellular functions of MCSs and the role of MCSs in disease will be addressed.

AUTHOR CONTRIBUTIONS

All authors listed have made a substantial, direct and intellectual contribution to the work, and approved it for publication.

FUNDING

This work was supported by the National Natural Science Foundation of China (Nos. 91854101 and 31801166) and the Natural Science Foundation of Chongqing, China (No. cstc2019jcyj-msxmX0257) and the Fundamental Research Funds for the Central Universities (Nos. 2018CDQYSM0037 and 2019CDCGSM303).

REFERENCES

Alford, S. C., Abdelfattah, A. S., Ding, Y., and Campbell, R. E. (2012a). A fluorogenic red fluorescent protein heterodimer. *Chem. Biol.* 19, 353–360. doi: 10.1016/j.chembiol.2012.01.006

Alford, S. C., Ding, Y., Simmen, T., and Campbell, R. E. (2012b). Dimerization-dependent green and yellow fluorescent proteins. *ACS Synth. Biol.* 1, 569–575. doi: 10.1021/sb300050j

Algar, W. R., Hildebrandt, N., Vogel, S. S., and Medintz, I. L. (2019). FRET as a biomolecular research tool - understanding its potential while avoiding pitfalls. *Nat. Methods* 16, 815–829. doi: 10.1038/s41592-019-0530-8

Allison, R., Edgar, J. R., Pearson, G., Rizo, T., Newton, T., Gunther, S., et al. (2017). Defects in ER-endosome contacts impact lysosome function in hereditary spastic paraplegia. *J. Cell Biol.* 216, 1337–1355. doi: 10.1083/jcb.201609033

Alpy, F., Rousseau, A., Schwab, Y., Legueux, F., Stoll, I., Wendling, C., et al. (2013). STARD3 or STARD3NL and VAP form a novel molecular tether between late endosomes and the ER. *J. Cell Sci.* 126(Pt 23), 5500–5512. doi: 10.1242/jcs.139295

Atakpa, P., Thillaiappan, N. B., Mataragka, S., Prole, D. L., and Taylor, C. W. (2018). IP3 receptors preferentially associate with ER-lysosome contact sites and selectively deliver Ca^{2+} to lysosomes. *Cell Rep.* 25, 3180–3193.e7. doi: 10.1016/j.celrep.2018.11.064

Balderhaar, H. J., and Ungermann, C. (2013). CORVET and HOPS tethering complexes - coordinators of endosome and lysosome fusion. *J. Cell Sci.* 126(Pt 6), 1307–1316. doi: 10.1242/jcs.107805

Bastiaens, P. I., and Squire, A. (1999). Fluorescence lifetime imaging microscopy: spatial resolution of biochemical processes in the cell. *Trends Cell Biol.* 9, 48–52. doi: 10.1016/s0962-8924(98)01410-x

Bernard-Marissal, N., Medard, J. J., Azzedine, H., and Chrast, R. (2015). Dysfunction in endoplasmic reticulum-mitochondria crosstalk underlies SIGMAR1 loss of function mediated motor neuron degeneration. *Brain* 138(Pt 4), 875–890. doi: 10.1093/brain/awv008

Bernhard, W., and Rouiller, C. (1956). Close topographical relationship between mitochondria and ergastoplasm of liver cells in a definite phase of cellular activity. *J. Biophys. Biochem. Cytol.* 2 (4 Suppl.), 73–78. doi: 10.1083/jcb.2.4.73

Bersuker, K., Peterson, C. W. H., To, M., Sahl, S. J., Savikhin, V., Grossman, E. A., et al. (2018). A proximity labeling strategy provides insights into the composition and dynamics of lipid droplet proteomes. *Dev. Cell* 44, 97–112.e7. doi: 10.1016/j.devcel.2017.11.020

Besprozvannaya, M., Dickson, E., Li, H., Ginburg, K. S., Bers, D. M., Auwerx, J., et al. (2018). GRAM domain proteins specialize functionally distinct ER-PM contact sites in human cells. *eLife* 7:e31019. doi: 10.7554/eLife.31019

Betzig, E., Patterson, G. H., Sougrat, R., Lindwasser, O. W., Olenych, S., Bonifacino, J. S., et al. (2006). Imaging intracellular fluorescent proteins at nanometer resolution. *Science* 313, 1642–1645. doi: 10.1126/science.1127344

Biazik, J., Yla-Anttila, P., Vihinen, H., Jokitalo, E., and Eskelinen, E. L. (2015). Ultrastructural relationship of the phagophore with surrounding organelles. *Autophagy* 11, 439–451. doi: 10.1080/15548627.2015.1017178

Binns, D., Januszewski, T., Chen, Y., Hill, J., Markin, V. S., Zhao, Y., et al. (2006). An intimate collaboration between peroxisomes and lipid bodies. *J. Cell Biol.* 173, 719–731. doi: 10.1083/jcb.200511125

Bockler, S., and Westermann, B. (2014). ER-mitochondria contacts as sites of mitophagosome formation. *Autophagy* 10, 1346–1347. doi: 10.4161/auto.28981

Branon, T. C., Bosch, J. A., Sanchez, A. D., Udeshi, N. D., Svinkina, T., Carr, S. A., et al. (2018). Efficient proximity labeling in living cells and organisms with TurboID. *Nat. Biotechnol.* 36, 880–887. doi: 10.1038/nbt.4201

Cabantous, S., Terwilliger, T. C., and Waldo, G. S. (2005). Protein tagging and detection with engineered self-assembling fragments of green fluorescent protein. *Nat. Biotechnol.* 23, 102–107. doi: 10.1038/nbt1044

Cacciagli, P., Sutera-Sardo, J., Borges-Correia, A., Roux, J. C., Dorboz, I., Desvignes, J. P., et al. (2013). Mutations in BCAP31 cause a severe X-linked phenotype with deafness, dystonia, and central hypomyelination and disorganize the Golgi apparatus. *Am. J. Hum. Genet.* 93, 579–586. doi: 10.1016/j.ajhg.2013.07.023

Chang, C. L., Chen, Y. J., Quintanilla, C. G., Hsieh, T. S., and Liou, J. (2018). EB1 binding restricts STIM1 translocation to ER-PM junctions and regulates store-operated Ca^{2+} entry. *J. Cell Biol.* 217, 2047–2058. doi: 10.1083/jcb.201711151

Chen, B. C., Legant, W. R., Wang, K., Shao, L., Milkie, D. E., Davidson, M. W., et al. (2014). Lattice light-sheet microscopy: imaging molecules to embryos at high spatiotemporal resolution. *Science* 346:1257998. doi: 10.1126/science.1257998

Chen, Y. J., Chang, C. L., Lee, W. R., and Liou, J. (2017). RASSF4 controls SOCE and ER-PM junctions through regulation of PI(4,5)P2. *J. Cell Biol.* 216, 2011–2025. doi: 10.1083/jcb.201606047

Cho, I. T., Adelmant, G., Lim, Y., Marto, J. A., Cho, G., and Golden, J. A. (2017). Ascorbate peroxidase proximity labeling coupled with biochemical fractionation identifies promoters of endoplasmic reticulum-mitochondrial contacts. *J. Biol. Chem.* 292, 16382–16392. doi: 10.1074/jbc.M117.795286

Chu, B. B., Liao, Y. C., Qi, W., Xie, C., Du, X., Wang, J., et al. (2015). Cholesterol transport through lysosome-peroxisome membrane contacts. *Cell* 161, 291–306. doi: 10.1016/j.cell.2015.02.019

Cieri, D., Vicario, M., Giacomello, M., Vallese, F., Filadi, R., Wagner, T., et al. (2018). SPLICS: a split green fluorescent protein-based contact site sensor for narrow and wide heterotypic organelle juxtaposition. *Cell Death Differ.* 25, 1131–1145. doi: 10.1038/s41418-017-0033-z

Cohen, S., Valm, A. M., and Lippincott-Schwartz, J. (2018). Interacting organelles. *Curr. Opin. Cell Biol.* 53, 84–91. doi: 10.1016/j.ceb.2018.06.003

Collado, J., and Fernandez-Busnadiego, R. (2017). Deciphering the molecular architecture of membrane contact sites by cryo-electron tomography. *Biochim. Biophys. Acta Mol. Cell Res.* 1864, 1507–1512. doi: 10.1016/j.bbamcr.2017.03.009

Copeland, D. E., and Dalton, A. J. (1959). An association between mitochondria and the endoplasmic reticulum in cells of the pseudobranch gland of a teleost. *J. Biophys. Biochem. Cytol.* 5, 393–396. doi: 10.1083/jcb.5.3.393

Costello, J. L., Castro, I. G., Schrader, T. A., Islinger, M., and Schrader, M. (2017). Peroxisomal ACBD4 interacts with VAPB and promotes ER-peroxisome associations. *Cell Cycle* 16, 1039–1045. doi: 10.1080/15384101.2017.1314422

Cronan, J. E. (2005). Targeted and proximity-dependent promiscuous protein biotinylation by a mutant *Escherichia coli* biotin protein ligase. *J. Nutr. Biochem.* 16, 416–418. doi: 10.1016/j.jnutbio.2005.03.017

Csordas, G., Renken, C., Varnai, P., Walter, L., Weaver, D., Buttle, K. F., et al. (2006). Structural and functional features and significance of the physical linkage between ER and mitochondria. *J. Cell Biol.* 174, 915–921. doi: 10.1083/jcb.200604016

Csordas, G., Varnai, P., Golenar, T., Roy, S., Purkins, G., Schneider, T. G., et al. (2010). Imaging interorganelle contacts and local calcium dynamics at the ER-mitochondrial interface. *Mol Cell* 39, 121–132. doi: 10.1016/j.molcel.2010.06.029

D'Angelo, G., Polishchuk, E., Di Tullio, G., Santoro, M., Di Campli, A., Godi, A., et al. (2007). Glycosphingolipid synthesis requires FAPP2 transfer of glucosylceramide. *Nature* 449, 62–67. doi: 10.1038/nature06097

De, A. (2011). The new era of bioluminescence resonance energy transfer technology. *Curr. Pharm. Biotechnol.* 12, 558–568. doi: 10.2174/138920111795163922

de Brito, O. M., and Scorrano, L. (2008). Mitofusin 2 tethers endoplasmic reticulum to mitochondria. *Nature* 456, 605–610. doi: 10.1038/nature07534

De Munter, S., Gornemann, J., Derua, R., Lesage, B., Qian, J., Heroes, E., et al. (2017). Split-BioID: a proximity biotinylation assay for dimerization-dependent protein interactions. *FEBS Lett.* 591, 415–424. doi: 10.1002/1873-3468.12548

De Vos, K. J., Morotz, G. M., Stoica, R., Tudor, E. L., Lau, K. F., Ackerley, S., et al. (2012). VAPB interacts with the mitochondrial protein PTPIP51 to regulate calcium homeostasis. *Hum. Mol. Genet.* 21, 1299–1311. doi: 10.1093/hmg/ddr559

D'Eletto, M., Rossin, F., Occhigrossi, L., Farrace, M. G., Faccenda, D., Desai, R., et al. (2018). Transglutaminase type 2 regulates ER-mitochondria contact sites by interacting with GRP75. *Cell Rep.* 25, 3573.e–3581.e. doi: 10.1016/j.celrep.2018.11.094

Ding, Y., Li, J., Enterina, J. R., Shen, Y., Zhang, I., Tewson, P. H., et al. (2015). Ratiometric biosensors based on dimerization-dependent fluorescent protein exchange. *Nat. Methods* 12, 195–198. doi: 10.1038/nmeth.3261

Dong, D., Huang, X., Li, L., Mao, H., Mo, Y., Zhang, G., et al. (2020). Super-resolution fluorescence-assisted diffraction computational tomography reveals the three-dimensional landscape of the cellular organelle interactome. *Light Sci. Appl.* 9:11. doi: 10.1038/s41377-020-0249-4

Dong, R., Saheki, Y., Swarup, S., Lucast, L., Harper, J. W., and De Camilli, P. (2016). Endosome-ER contacts control actin nucleation and retromer function through VAP-dependent regulation of PI4P. *Cell* 166, 408–423. doi: 10.1016/j.cell.2016.06.037

Drobne, D. (2013). 3D imaging of cells and tissues by focused ion beam/scanning electron microscopy (FIB/SEM). *Methods Mol. Biol.* 950, 275–292. doi: 10.1007/978-1-62703-137-0_16

Du, X., Kumar, J., Ferguson, C., Schulz, T. A., Ong, Y. S., Hong, W., et al. (2011). A role for oxysterol-binding protein-related protein 5 in endosomal cholesterol trafficking. *J. Cell Biol.* 192, 121–135. doi: 10.1083/jcb.201004142

Dugail, I. (2014). Lysosome/lipid droplet interplay in metabolic diseases. *Biochimie* 96, 102–105. doi: 10.1016/j.biochi.2013.07.008

Eden, E. R., White, I. J., Tsapara, A., and Futter, C. E. (2010). Membrane contacts between endosomes and ER provide sites for PTP1B-epidermal growth factor receptor interaction. *Nat. Cell Biol.* 12, 267–272. doi: 10.1038/ncb2026

Eisenberg-Bord, M., Shai, N., Schuldiner, M., and Bohnert, M. (2016). A tether is a tether is a tether: tethering at membrane contact sites. *Dev. Cell* 39, 395–409. doi: 10.1016/j.devcel.2016.10.022

Elangovan, M., Day, R. N., and Periasamy, A. (2002). Nanosecond fluorescence resonance energy transfer-fluorescence lifetime imaging microscopy to localize the protein interactions in a single living cell. *J. Microsc.* 205(Pt 1), 3–14. doi: 10.1046/j.0022-2720.2001.00984.x

Elbaz-Alon, Y., Eisenberg-Bord, M., Shinder, V., Stiller, S. B., Shimoni, E., Wiedemann, N., et al. (2015). Lam6 regulates the extent of contacts between organelles. *Cell Rep.* 12, 7–14. doi: 10.1016/j.celrep.2015.06.022

Feng, S., Sekine, S., Pessino, V., Li, H., Leonetti, M. D., and Huang, B. (2017). Improved split fluorescent proteins for endogenous protein labeling. *Nat. Commun.* 8:370. doi: 10.1038/s41467-017-00494-8

Fermie, J., Liv, N., Ten Brink, C., van Donselaar, E. G., Muller, W. H., Schieber, N. L., et al. (2018). Single organelle dynamics linked to 3D structure by correlative live-cell imaging and 3D electron microscopy. *Traffic* 19, 354–369. doi: 10.1111/tra.12557

Fernandez-Busnadiego, R. (2016). Supramolecular architecture of endoplasmic reticulum-plasma membrane contact sites. *Biochem. Soc. Trans.* 44, 534–540. doi: 10.1042/BST20150279

Fernandez-Busnadiego, R., Saheki, Y., and De Camilli, P. (2015). Three-dimensional architecture of extended synaptotagmin-mediated endoplasmic reticulum-plasma membrane contact sites. *Proc. Natl. Acad. Sci. U.S.A.* 112, E2004–E2013. doi: 10.1073/pnas.1503191112

Fredriksson, S., Dixon, W., Ji, H., Koong, A. C., Mindrinos, M., and Davis, R. W. (2007). Multiplexed protein detection by proximity ligation for cancer biomarker validation. *Nat. Methods* 4, 327–329. doi: 10.1038/nmeth1020

Fredriksson, S., Gullberg, M., Jarvius, J., Olsson, C., Pietras, K., Gustafsdottir, S. M., et al. (2002). Protein detection using proximity-dependent DNA ligation assays. *Nat. Biotechnol.* 20, 473–477. doi: 10.1038/nbt0502-473

Friedman, J. R., Lackner, L. L., West, M., DiBenedetto, J. R., Nunnari, J., and Voeltz, G. K. (2011). ER tubules mark sites of mitochondrial division. *Science* 334, 358–362. doi: 10.1126/science.1207385

Galarneau, A., Primeau, M., Trudeau, L. E., and Michnick, S. W. (2002). Beta-lactamase protein fragment complementation assays as *in vivo* and *in vitro* sensors of protein protein interactions. *Nat. Biotechnol.* 20, 619–622. doi: 10.1038/nbt0602-619

Galiani, S., Waithe, D., Reglinski, K., Cruz-Zaragoza, L. D., Garcia, E., Clausen, M. P., et al. (2016). Super-resolution microscopy reveals compartmentalization of peroxisomal membrane proteins. *J. Biol. Chem.* 291, 16948–16962. doi: 10.1074/jbc.M116.734038

Garofalo, T., Matarrese, P., Manganelli, V., Marconi, M., Tinari, A., Gambardella, L., et al. (2016). Evidence for the involvement of lipid rafts localized at

the ER-mitochondria associated membranes in autophagosome formation. *Autophagy* 12, 917–935. doi: 10.1080/15548627.2016.1160971

Gingras, A. C., Abe, K. T., and Raught, B. (2019). Getting to know the neighborhood: using proximity-dependent biotinylation to characterize protein complexes and map organelles. *Curr. Opin. Chem. Biol.* 48, 44–54. doi: 10.1016/j.cbpa.2018.10.017

Gomez-Suaga, P., Paillusson, S., Stoica, R., Noble, W., Hanger, D. P., and Miller, C. C. J. (2017). The ER-mitochondria tethering complex VAPB-PTPIP51 regulates autophagy. *Curr. Biol.* 27, 371–385. doi: 10.1016/j.cub.2016.12.038

Gonzalez Montoro, A., Auffarth, K., Honscher, C., Bohnert, M., Becker, T., Warscheid, B., et al. (2018). Vps39 interacts with Tom40 to establish one of two functionally distinct vacuole-mitochondria contact sites. *Dev. Cell* 45, 621–636.e7. doi: 10.1016/j.devcel.2018.05.011

Gould, T. J., Verkhusha, V. V., and Hess, S. T. (2009). Imaging biological structures with fluorescence photoactivation localization microscopy. *Nat. Protoc.* 4, 291–308. doi: 10.1038/nprot.2008.246

Guo, M., Chandris, P., Giannini, J. P., Trexler, A. J., Fischer, R., Chen, J., et al. (2018). Single-shot super-resolution total internal reflection fluorescence microscopy. *Nat. Methods* 15, 425–428. doi: 10.1038/s41592-018-0004-4

Guo, Y., Li, D., Zhang, S., Yang, Y., Liu, J. J., Wang, X., et al. (2018). Visualizing intracellular organelle and cytoskeletal interactions at nanoscale resolution on millisecond timescales. *Cell* 175, 1430–1442.e17. doi: 10.1016/j.cell.2018.09.057

Gupta, G. D., Coyaud, E., Goncalves, J., Mojarad, B. A., Liu, Y., Wu, Q., et al. (2015). A dynamic protein interaction landscape of the human centrosome-cilium interface. *Cell* 163, 1484–1499. doi: 10.1016/j.cell.2015.10.065

Hamasaki, M., Furuta, N., Matsuda, A., Nezu, A., Yamamoto, A., Fujita, N., et al. (2013). Autophagosomes form at ER-mitochondria contact sites. *Nature* 495, 389–393. doi: 10.1038/nature11910

Han, Y., Branon, T. C., Martell, J. D., Boassa, D., Shechner, D., Ellisman, M. H., et al. (2019). Directed evolution of split APEX2 peroxidase. *ACS Chem. Biol.* 14, 619–635. doi: 10.1021/acschembio.8b00919

Hanada, K., Kumagai, K., Yasuda, S., Miura, Y., Kawano, M., Fukasawa, M., et al. (2003). Molecular machinery for non-vesicular trafficking of ceramide. *Nature* 426, 803–809. doi: 10.1038/nature02188

Hao, F., Kondo, K., Itoh, T., Ikari, S., Nada, S., Okada, M., et al. (2018). Rheb localized on the Golgi membrane activates lysosome-localized mTORC1 at the Golgi-lysosome contact site. *J. Cell Sci.* 131:jcs208017. doi: 10.1242/jcs.208017

Hayashi, T., Rizzuto, R., Hajnoczky, G., and Su, T. P. (2009). MAM: more than just a housekeeper. *Trends Cell Biol.* 19, 81–88. doi: 10.1016/j.tcb.2008.12.002

Helle, S. C., Kanfer, G., Kolar, K., Lang, A., Michel, A. H., and Kornmann, B. (2013). Organization and function of membrane contact sites. *Biochim. Biophys. Acta* 1833, 2526–2541. doi: 10.1016/j.bbamcr.2013.01.028

Henne, W. M., Zhu, L., Balogi, Z., Stefan, C., Pleiss, J. A., and Emr, S. D. (2015). Mdm1/Snx13 is a novel ER-endolysosomal interorganelle tethering protein. *J. Cell Biol.* 210, 541–551. doi: 10.1083/jcb.201503088

Hertlein, V., Flores-Romero, H., Das, K. K., Fischer, S., Heunemann, M., Calleja-Felipe, M., et al. (2020). MERLIN: a novel BRET-based proximity biosensor for studying mitochondria-ER contact sites. *Life Sci. Alliance* 3:e201900600. doi: 10.26508/lsa.201900600

Honscher, C., Mari, M., Auffarth, K., Bohnert, M., Griffith, J., Geerts, W., et al. (2014). Cellular metabolism regulates contact sites between vacuoles and mitochondria. *Dev. Cell* 30, 86–94. doi: 10.1016/j.devcel.2014.06.006

Hoyer, M. J., Chitwood, P. J., Ebmeier, C. C., Striepen, J. F., Qi, R. Z., Old, W. M., et al. (2018). A novel class of ER membrane proteins regulates ER-associated endosome fission. *Cell* 175, 254–265.e14. doi: 10.1016/j.cell.2018.08.030

Hsieh, T. S., Chen, Y. J., Chang, C. L., Lee, W. R., and Liou, J. (2017). Cortical actin contributes to spatial organization of ER-PM junctions. *Mol. Biol. Cell* 28, 3171–3180. doi: 10.1091/mbc.E17-06-0377

Hsu, F., Spannl, S., Ferguson, C., Hyman, A. A., Parton, R. G., and Zerial, M. (2018). Rab5 and Alsin regulate stress-activated cytoprotective signaling on mitochondria. *eLife* 7:e32282. doi: 10.7554/eLife.32282

Hua, R., Cheng, D., Coyaud, E., Freeman, S., Di Pietro, E., Wang, Y., et al. (2017). VAPs and ACBD5 tether peroxisomes to the ER for peroxisome maintenance and lipid homeostasis. *J. Cell Biol.* 216, 367–377. doi: 10.1083/jcb.201608128

Hua, R., Gidda, S. K., Aranovich, A., Mullen, R. T., and Kim, P. K. (2015). Multiple domains in PEX16 mediate its trafficking and recruitment of peroxisomal proteins to the ER. *Traffic* 16, 832–852. doi: 10.1111/tra.12292

Huang, X., Fan, J., Li, L., Liu, H., Wu, R., Wu, Y., et al. (2018). Fast, long-term, super-resolution imaging with Hessian structured illumination microscopy. *Nat. Biotechnol.* 36, 451–459. doi: 10.1038/nbt.4115

Hung, V., Lam, S. S., Udeshi, N. D., Svinkina, T., Guzman, G., Mootha, V. K., et al. (2017). Proteomic mapping of cytosol-facing outer mitochondrial and ER membranes in living human cells by proximity biotinylation. *eLife* 6:e24463. doi: 10.7554/eLife.24463

Hung, V., Zou, P., Rhee, H. W., Udeshi, N. D., Cracan, V., Svinkina, T., et al. (2014). Proteomic mapping of the human mitochondrial intermembrane space in live cells via ratiometric APEX tagging. *Mol. Cell* 55, 332–341. doi: 10.1016/j.molcel.2014.06.003

Inoue, T., Heo, W. D., Grimley, J. S., Wandless, T. J., and Meyer, T. (2005). An inducible translocation strategy to rapidly activate and inhibit small GTPase signaling pathways. *Nat. Methods* 2, 415–418. doi: 10.1038/nmeth763

Iwasawa, R., Mahul-Mellier, A. L., Datler, C., Pazarentzos, E., and Grimm, S. (2011). Fis1 and Bap31 bridge the mitochondria-ER interface to establish a platform for apoptosis induction. *EMBO J.* 30, 556–568. doi: 10.1038/emboj.2010.346

Jamecna, D., Polidori, J., Mesmin, B., Dezi, M., Levy, D., Bigay, J., et al. (2019). An intrinsically disordered region in OSBP acts as an entropic barrier to control protein dynamics and orientation at membrane contact sites. *Dev. Cell* 49, 220–234.e8. doi: 10.1016/j.devcel.2019.02.021

Jansen, M., Ohsaki, Y., Rega, L. R., Bittman, R., Olkkonen, V. M., and Ikonen, E. (2011). Role of ORPs in sterol transport from plasma membrane to ER and lipid droplets in mammalian cells. *Traffic* 12, 218–231. doi: 10.1111/j.1600-0854.2010.01142.x

Jardin, I., Lopez, J. J., Salido, G. M., and Rosado, J. A. (2008). Orai1 mediates the interaction between STIM1 and hTRPC1 and regulates the mode of activation of hTRPC1-forming Ca^{2+} channels. *J. Biol. Chem.* 283, 25296–25304. doi: 10.1074/jbc.M802904200

Jiang, P., Nishimura, T., Sakamaki, Y., Itakura, E., Hatta, T., Natsume, T., et al. (2014). The HOPS complex mediates autophagosome-lysosome fusion through interaction with syntaxin 17. *Mol. Biol. Cell* 25, 1327–1337. doi: 10.1091/mbc.E13-08-0447

Jing, J., He, L., Sun, A., Quintana, A., Ding, Y., Ma, G., et al. (2015). Proteomic mapping of ER-PM junctions identifies STIMATE as a regulator of Ca^{2+} influx. *Nat. Cell Biol.* 17, 1339–1347. doi: 10.1038/ncb3234

Jing, J., Liu, G., Huang, Y., and Zhou, Y. (2019). A molecular toolbox for interrogation of membrane contact sites. *J. Physiol.* doi: 10.1113/JP277761 [Epub ahead of print].

Johnsson, N., and Varshavsky, A. (1994). Split ubiquitin as a sensor of protein interactions *in vivo*. *Proc. Natl. Acad. Sci. U.S.A.* 91, 10340–10344. doi: 10.1073/pnas.91.22.10340

Joshi, A. S., Nebenfuehr, B., Choudhary, V., Satpute-Krishnan, P., Levine, T. P., Golden, A., et al. (2018). Lipid droplet and peroxisome biogenesis occur at the same ER subdomains. *Nat. Commun.* 9:2940. doi: 10.1038/s41467-018-05277-3

Kakimoto, Y., Tashiro, S., Kojima, R., Morozumi, Y., Endo, T., and Tamura, Y. (2018). Visualizing multiple inter-organelle contact sites using the organelle-targeted split-GFP system. *Sci. Rep.* 8:6175. doi: 10.1038/s41598-018-24466-0

Kang, F., Zhou, M., Huang, X., Fan, J., Wei, L., Boulanger, J., et al. (2019). E-syt1 Re-arranges STIM1 clusters to stabilize ring-shaped ER-PM contact sites and accelerate Ca^{2+} store replenishment. *Sci. Rep.* 9:3975. doi: 10.1038/s41598-019-40331-0

Kawamata, H., Peixoto, P., Konrad, C., Palomo, G., Bredvik, K., Gerges, M., et al. (2017). Mutant TDP-43 does not impair mitochondrial bioenergetics *in vitro* and *in vivo*. *Mol. Neurodegener.* 12:37. doi: 10.1186/s13024-017-0180-1

Kawano, S., Tamura, Y., Kojima, R., Bala, S., Asai, E., Michel, A. H., et al. (2018). Structure-function insights into direct lipid transfer between membranes by Mmm1-Mdm12 of ERMES. *J. Cell Biol.* 217, 959–974. doi: 10.1083/jcb.201704119

Kim, D. I., Birendra, K. C., Zhu, W., Motamedchaboki, K., Doye, V., and Roux, K. J. (2014). Probing nuclear pore complex architecture with proximity-dependent biotinylation. *Proc. Natl. Acad. Sci. U.S.A.* 111, E2453–E2461. doi: 10.1073/pnas.1406459111

Kim, Y. J., Guzman-Hernandez, M. L., Wisniewski, E., and Balla, T. (2015). Phosphatidylinositol-Phosphatidic acid exchange by Nir2 at ER-PM contact sites maintains phosphoinositide signaling competence. *Dev. Cell* 33, 549–561. doi: 10.1016/j.devcel.2015.04.028

Kirisako, T., Baba, M., Ishihara, N., Miyazawa, K., Ohsumi, M., Yoshimori, T., et al. (1999). Formation process of autophagosome is traced with Apg8/Aut7p in yeast. *J. Cell Biol.* 147, 435–446. doi: 10.1083/jcb.147.2.435

Kner, P., Chhun, B. B., Griffis, E. R., Winoto, L., and Gustafsson, M. G. (2009). Super-resolution video microscopy of live cells by structured illumination. *Nat. Methods* 6, 339–342. doi: 10.1038/nmeth.1324

Knoblach, B., Sun, X., Coquelle, N., Fagarasanu, A., Poirier, R. L., and Rachubinski, R. A. (2013). An ER-peroxisome tether exerts peroxisome population control in yeast. *EMBO J.* 32, 2439–2453. doi: 10.1038/emboj.2013.170

Kornmann, B., Currie, E., Collins, S. R., Schuldiner, M., Nunnari, J., Weissman, J. S., et al. (2009). An ER-mitochondria tethering complex revealed by a synthetic biology screen. *Science* 325, 477–481. doi: 10.1126/science.1175088

Kornmann, B., Osman, C., and Walter, P. (2011). The conserved GTPase Gem1 regulates endoplasmic reticulum-mitochondria connections. *Proc. Natl. Acad. Sci. U.S.A.* 108, 14151–14156. doi: 10.1073/pnas.1111314108

Krols, M., van Isterdael, G., Asselbergh, B., Kremer, A., Lippens, S., Timmerman, V., et al. (2016). Mitochondria-associated membranes as hubs for neurodegeneration. *Acta Neuropathol.* 131, 505–523. doi: 10.1007/s00401-015-1528-7

Kvam, E., and Goldfarb, D. S. (2006). Nucleus-vacuole junctions in yeast: anatomy of a membrane contact site. *Biochem. Soc. Trans.* 34(Pt 3), 340–342. doi: 10.1042/BST0340340

Lackner, L. L., Ping, H., Graef, M., Murley, A., and Nunnari, J. (2013). Endoplasmic reticulum-associated mitochondria-cortex tether functions in the distribution and inheritance of mitochondria. *Proc. Natl. Acad. Sci. U.S.A.* 110, E458–E467. doi: 10.1073/pnas.1215232110

Lahiri, S., Chao, J. T., Tavassoli, S., Wong, A. K., Choudhary, V., Young, B. P., et al. (2014). A conserved endoplasmic reticulum membrane protein complex (EMC) facilitates phospholipid transfer from the ER to mitochondria. *PLoS Biol.* 12:e1001969. doi: 10.1371/journal.pbio.1001969

Lahiri, S., Toulmay, A., and Prinz, W. A. (2015). Membrane contact sites, gateways for lipid homeostasis. *Curr. Opin. Cell Biol.* 33, 82–87. doi: 10.1016/j.ceb.2014.12.004

Lam, S. S., Martell, J. D., Kamer, K. J., Deerinck, T. J., Ellisman, M. H., Mootha, V. K., et al. (2015). Directed evolution of APEX2 for electron microscopy and proximity labeling. *Nat. Methods* 12, 51–54. doi: 10.1038/nmeth.3179

Landstrom, A. P., Weisleder, N., Batalden, K. B., Bos, J. M., Tester, D. J., Ommen, S. R., et al. (2007). Mutations in JPH2-encoded junctophilin-2 associated with hypertrophic cardiomyopathy in humans. *J. Mol. Cell. Cardiol.* 42, 1026–1035. doi: 10.1016/j.yjmcc.2007.04.006

Lane, M. D., Young, D. L., and Lynen, F. (1964). The enzymatic synthesis of holotranscarboxylase from apotranscarboxylase and (+)-Biotin. I. Purification of the apoenzyme and synthetase; characteristics of the reaction. *J. Biol. Chem.* 239, 2858–2864.

Lawrence, B. P., and Brown, W. J. (1992). Autophagic vacuoles rapidly fuse with pre-existing lysosomes in cultured hepatocytes. *J. Cell Sci.* 102(Pt 3), 515–526.

Lawrence, R. E., and Zoncu, R. (2019). The lysosome as a cellular centre for signalling, metabolism and quality control. *Nat. Cell Biol.* 21, 133–142. doi: 10.1038/s41556-018-0244-7

Levine, T. P., and Munro, S. (2001). Dual targeting of Osh1p, a yeast homologue of oxysterol-binding protein, to both the Golgi and the nucleus-vacuole junction. *Mol. Biol. Cell* 12, 1633–1644. doi: 10.1091/mbc.12.6.1633

Li, D., Shao, L., Chen, B. C., Zhang, X., Zhang, M., Moses, B., et al. (2015). Extended-resolution structured illumination imaging of endocytic and cytoskeletal dynamics. *Science* 349:aab3500. doi: 10.1126/science.aab3500

Lim, Y., Cho, I. T., Schoel, L. J., Cho, G., and Golden, J. A. (2015). Hereditary spastic paraplegia-linked REEP1 modulates endoplasmic reticulum/mitochondria contacts. *Ann. Neurol.* 78, 679–696. doi: 10.1002/ana.24488

Liou, J., Fivaz, M., Inoue, T., and Meyer, T. (2007). Live-cell imaging reveals sequential oligomerization and local plasma membrane targeting of stromal interaction molecule 1 after Ca^{2+} store depletion. *Proc. Natl. Acad. Sci. U.S.A.* 104, 9301–9306. doi: 10.1073/pnas.0702866104

Litvak, V., Dahan, N., Ramachandran, S., Sabanay, H., and Lev, S. (2005). Maintenance of the diacylglycerol level in the Golgi apparatus by the Nir2 protein is critical for Golgi secretory function. *Nat. Cell Biol.* 7, 225–234. doi: 10.1038/ncb1221

Liu, L. K., Choudhary, V., Toulmay, A., and Prinz, W. A. (2017). An inducible ER-Golgi tether facilitates ceramide transport to alleviate lipotoxicity. *J. Cell Biol.* 216, 131–147. doi: 10.1083/jcb.201606059

Luker, K. E., Smith, M. C., Luker, G. D., Gammon, S. T., Piwnica-Worms, H., and Piwnica-Worms, D. (2004). Kinetics of regulated protein-protein interactions revealed with firefly luciferase complementation imaging in cells and living animals. *Proc. Natl. Acad. Sci. U.S.A.* 101, 12288–12293. doi: 10.1073/pnas.0404041101

Magliery, T. J., Wilson, C. G., Pan, W., Mishler, D., Ghosh, I., Hamilton, A. D., et al. (2005). Detecting protein-protein interactions with a green fluorescent protein fragment reassembly trap: scope and mechanism. *J. Am. Chem. Soc.* 127, 146–157. doi: 10.1021/ja046699g

Mair, A., Xu, S. L., Branon, T. C., Ting, A. Y., and Bergmann, D. C. (2019). Proximity labeling of protein complexes and cell-type-specific organellar proteomes in Arabidopsis enabled by TurboID. *eLife* 8:e47864. doi: 10.7554/eLife.47864

Manford, A. G., Stefan, C. J., Yuan, H. L., Macgurn, J. A., and Emr, S. D. (2012). ER-to-plasma membrane tethering proteins regulate cell signaling and ER morphology. *Dev. Cell* 23, 1129–1140. doi: 10.1016/j.devcel.2012.11.004

Martell, J. D., Deerinck, T. J., Sancak, Y., Poulos, T. L., Mootha, V. K., Sosinsky, G. E., et al. (2012). Engineered ascorbate peroxidase as a genetically encoded reporter for electron microscopy. *Nat. Biotechnol.* 30, 1143–1148. doi: 10.1038/nbt.2375

Marx, V. (2017). Probes: FRET sensor design and optimization. *Nat. Methods* 14, 949–953. doi: 10.1038/nmeth.4434

Mc Donald, J. M., and Krainc, D. (2017). Lysosomal proteins as a therapeutic target in neurodegeneration. *Annu. Rev. Med.* 68, 445–458. doi: 10.1146/annurev-med-050715-104432

Mesmin, B., Bigay, J., Moser von Filseck, J., Lacas-Gervais, S., Drin, G., and Antonny, B. (2013). A four-step cycle driven by PI(4)P hydrolysis directs sterol/PI(4)P exchange by the ER-Golgi tether OSBP. *Cell* 155, 830–843. doi: 10.1016/j.cell.2013.09.056

Mitchell, A. C., Alford, S. C., Hunter, S. A., Kannan, D., Parra Sperberg, R. A., Chang, C. H., et al. (2018). Development of a protease biosensor based on a dimerization-dependent red fluorescent protein. *ACS Chem. Biol.* 13, 66–72. doi: 10.1021/acschembio.7b00715

Miyawaki, A., Llopis, J., Heim, R., McCaffery, J. M., Adams, J. A., Ikura, M., et al. (1997). Fluorescent indicators for Ca^{2+} based on green fluorescent proteins and calmodulin. *Nature* 388, 882–887. doi: 10.1038/42264

Mo, X. L., and Fu, H. (2016). BRET: nanoluc-based bioluminescence resonance energy transfer platform to monitor protein-protein interactions in live cells. *Methods Mol. Biol.* 1439, 263–271. doi: 10.1007/978-1-4939-3673-1_17

Modi, S., Lopez-Domenech, G., Halff, E. F., Covill-Cooke, C., Ivankovic, D., Melandri, D., et al. (2019). Miro clusters regulate ER-mitochondria contact sites and link cristae organization to the mitochondrial transport machinery. *Nat. Commun.* 10:4399. doi: 10.1038/s41467-019-12382-4

Mullock, B. M., Smith, C. W., Ihrke, G., Bright, N. A., Lindsay, M., Parkinson, E. J., et al. (2000). Syntaxin 7 is localized to late endosome compartments, associates with Vamp 8, and Is required for late endosome-lysosome fusion. *Mol. Biol. Cell* 11, 3137–3153. doi: 10.1091/mbc.11.9.3137

Murley, A., Sarsam, R. D., Toulmay, A., Yamada, J., Prinz, W. A., and Nunnari, J. (2015). Ltc1 is an ER-localized sterol transporter and a component of ER-mitochondria and ER-vacuole contacts. *J. Cell Biol.* 209, 539–548. doi: 10.1083/jcb.201502033

Naon, D., and Scorrano, L. (2014). At the right distance: ER-mitochondria juxtaposition in cell life and death. *Biochim. Biophys. Acta* 1843, 2184–2194. doi: 10.1016/j.bbamcr.2014.05.011

Naon, D., Zaninello, M., Giacomello, M., Varanita, T., Grespi, F., Lakshminaranayan, S., et al. (2016). Critical reappraisal confirms that Mitofusin 2 is an endoplasmic reticulum-mitochondria tether. *Proc. Natl. Acad. Sci. U.S.A.* 113, 11249–11254. doi: 10.1073/pnas.1606786113

Nascimbeni, A. C., Giordano, F., Dupont, N., Grasso, D., Vaccaro, M. I., Codogno, P., et al. (2017). ER-plasma membrane contact sites contribute to autophagosome biogenesis by regulation of local PI3P synthesis. *EMBO J.* 36, 2018–2033. doi: 10.15252/embj.201797006

Nishimura, A. L., Mitne-Neto, M., Silva, H. C., Richieri-Costa, A., Middleton, S., Cascio, D., et al. (2004). A mutation in the vesicle-trafficking protein VAPB

causes late-onset spinal muscular atrophy and amyotrophic lateral sclerosis. *Am. J. Hum. Genet.* 75, 822–831. doi: 10.1086/425287

Nixon-Abell, J., Obara, C. J., Weigel, A. V., Li, D., Legant, W. R., Xu, C. S., et al. (2016). Increased spatiotemporal resolution reveals highly dynamic dense tubular matrices in the peripheral ER. *Science* 354:aaf3928. doi: 10.1126/science.aaf3928

Nordmann, M., Cabrera, M., Perz, A., Brocker, C., Ostrowicz, C., Engelbrecht-Vandre, S., et al. (2010). The Mon1-Ccz1 complex is the GEF of the late endosomal Rab7 homolog Ypt7. *Curr. Biol.* 20, 1654–1659. doi: 10.1016/j.cub.2010.08.002

Ohashi, M., Miwako, I., Nakamura, K., Yamamoto, A., Murata, M., Ohnishi, S., et al. (1999). An arrested late endosome-lysosome intermediate aggregate observed in a Chinese hamster ovary cell mutant isolated by novel three-step screening. *J. Cell Sci.* 112(Pt 8), 1125–1138.

Olzmann, J. A., and Carvalho, P. (2019). Dynamics and functions of lipid droplets. *Nat. Rev. Mol. Cell Biol.* 20, 137–155. doi: 10.1038/s41580-018-0085-z

Ouasti, S., Matarrese, P., Paddon, R., Khosravi-Far, R., Sorice, M., Tinari, A., et al. (2007). Death receptor ligation triggers membrane scrambling between Golgi and mitochondria. *Cell Death Differ.* 14, 453–461. doi: 10.1038/sj.cdd.4402043

Paillusson, S., Stoica, R., Gomez-Suaga, P., Lau, D. H. W., Mueller, S., Miller, T., et al. (2016). There's Something Wrong with my MAM; the ER-Mitochondria Axis and Neurodegenerative Diseases. *Trends Neurosci.* 39, 146–157. doi: 10.1016/j.tins.2016.01.008

Palande, K., Roovers, O., Gits, J., Verwijmeren, C., Iuchi, Y., Fujii, J., et al. (2011). Peroxiredoxin-controlled G-CSF signalling at the endoplasmic reticulum-early endosome interface. *J. Cell Sci.* 124(Pt 21), 3695–3705. doi: 10.1242/jcs.089656

Pan, X., Roberts, P., Chen, Y., Kvam, E., Shulga, N., Huang, K., et al. (2000). Nucleus-vacuole junctions in Saccharomyces cerevisiae are formed through the direct interaction of Vac8p with Nvj1p. *Mol. Biol. Cell* 11, 2445–2457. doi: 10.1091/mbc.11.7.2445

Perroy, J., Pontier, S., Charest, P. G., Aubry, M., and Bouvier, M. (2004). Real-time monitoring of ubiquitination in living cells by BRET. *Nat. Methods* 1, 203–208. doi: 10.1038/nmeth722

Pfleger, K. D. G., and Eidne, K. A. (2006). Illuminating insights into protein-protein interactions using bioluminescence resonance energy transfer (BRET). *Nat. Methods* 3, 165–174. doi: 10.1038/nmeth841

Pietraszewska-Bogiel, A., and Gadella, T. W. (2011). FRET microscopy: from principle to routine technology in cell biology. *J. Microsc.* 241, 111–118. doi: 10.1111/j.1365-2818.2010.03437.x

Ponka, P., Sheftel, A. D., and Zhang, A. S. (2002). Iron targeting to mitochondria in erythroid cells. *Biochem. Soc. Trans.* 30, 735–738. doi: 10.1042/bst0300735

Porter, K. R., and Palade, G. E. (1957). Studies on the endoplasmic reticulum. III. Its form and distribution in striated muscle cells. *J. Biophys. Biochem. Cytol.* 3, 269–300. doi: 10.1083/jcb.3.2.269

Poteser, M., Leitinger, G., Pritz, E., Platzer, D., Frischauf, I., Romanin, C., et al. (2016). Live-cell imaging of ER-PM contact architecture by a novel TIRFM approach reveals extension of junctions in response to store-operated Ca^{2+}-entry. *Sci. Rep.* 6:35656. doi: 10.1038/srep35656

Prinz, W. A. (2014). Bridging the gap: membrane contact sites in signaling, metabolism, and organelle dynamics. *J. Cell Biol.* 205, 759–769. doi: 10.1083/jcb.201401126

Prinz, W. A., Toulmay, A., and Balla, T. (2020). The functional universe of membrane contact sites. *Nat. Rev. Mol. Cell Biol.* 21, 7–24. doi: 10.1038/s41580-019-0180-9

Raiborg, C., Wenzel, E. M., Pedersen, N. M., Olsvik, H., Schink, K. O., Schultz, S. W., et al. (2015). Repeated ER-endosome contacts promote endosome translocation and neurite outgrowth. *Nature* 520, 234–238. doi: 10.1038/nature14359

Rainey, K. H., and Patterson, G. H. (2019). Photoswitching FRET to monitor protein-protein interactions. *Proc. Natl. Acad. Sci. U.S.A.* 116, 864–873. doi: 10.1073/pnas.1805333116

Rekas, A., Alattia, J. R., Nagai, T., Miyawaki, A., and Ikura, M. (2002). Crystal structure of venus, a yellow fluorescent protein with improved maturation and reduced environmental sensitivity. *J. Biol. Chem.* 277, 50573–50578. doi: 10.1074/jbc.M209524200

Rhee, H. W., Zou, P., Udeshi, N. D., Martell, J. D., Mootha, V. K., Carr, S. A., et al. (2013). Proteomic mapping of mitochondria in living cells via spatially restricted enzymatic tagging. *Science* 339, 1328–1331. doi: 10.1126/science.1230593

Rizzuto, R., Brini, M., De Giorgi, F., Rossi, R., Heim, R., Tsien, R. Y., et al. (1996). Double labelling of subcellular structures with organelle-targeted GFP mutants in vivo. *Curr. Biol.* 6, 183–188. doi: 10.1016/s0960-9822(02)00451-7

Rizzuto, R., Brini, M., Murgia, M., and Pozzan, T. (1993). Microdomains with high Ca^{2+} close to IP3-sensitive channels that are sensed by neighboring mitochondria. *Science* 262, 744–747. doi: 10.1126/science.8235595

Rizzuto, R., Pinton, P., Carrington, W., Fay, F. S., Fogarty, K. E., Lifshitz, L. M., et al. (1998). Close contacts with the endoplasmic reticulum as determinants of mitochondrial Ca2+ responses. *Science* 280, 1763–1766. doi: 10.1126/science.280.5370.1763

Robenek, H., Hofnagel, O., Buers, I., Robenek, M. J., Troyer, D., and Severs, N. J. (2006). Adipophilin-enriched domains in the ER membrane are sites of lipid droplet biogenesis. *J. Cell Sci.* 119(Pt 20), 4215–4224. doi: 10.1242/jcs.03191

Rocha, N., Kuijl, C., van der Kant, R., Janssen, L., Houben, D., Janssen, H., et al. (2009). Cholesterol sensor ORP1L contacts the ER protein VAP to control Rab7-RILP-p150 Glued and late endosome positioning. *J. Cell Biol.* 185, 1209–1225. doi: 10.1083/jcb.200811005

Romoser, V. A., Hinkle, P. M., and Persechini, A. (1997). Detection in living cells of Ca^{2+}-dependent changes in the fluorescence emission of an indicator composed of two green fluorescent protein variants linked by a calmodulin-binding sequence. A new class of fluorescent indicators. *J. Biol. Chem.* 272, 13270–13274. doi: 10.1074/jbc.272.20.13270

Rust, M. J., Bates, M., and Zhuang, X. (2006). Sub-diffraction-limit imaging by stochastic optical reconstruction microscopy (STORM). *Nat. Methods* 3, 793–795. doi: 10.1038/nmeth929

Schallmeiner, E., Oksanen, E., Ericsson, O., Spangberg, L., Eriksson, S., Stenman, U. H., et al. (2007). Sensitive protein detection via triple-binder proximity ligation assays. *Nat. Methods* 4, 135–137. doi: 10.1038/nmeth974

Schauder, C. M., Wu, X., Saheki, Y., Narayanaswamy, P., Torta, F., Wenk, M. R., et al. (2014). Structure of a lipid-bound extended synaptotagmin indicates a role in lipid transfer. *Nature* 510, 552–555. doi: 10.1038/nature13269

Schneider, J., Zahn, J., Maglione, M., Sigrist, S. J., Marquard, J., Chojnacki, J., et al. (2015). Ultrafast, temporally stochastic STED nanoscopy of millisecond dynamics. *Nat. Methods* 12, 827–830. doi: 10.1038/nmeth.3481

Schon, E. A., and Area-Gomez, E. (2013). Mitochondria-associated ER membranes in Alzheimer disease. *Mol. Cell. Neurosci.* 55, 26–36. doi: 10.1016/j.mcn.2012.07.011

Schrader, M., and Yoon, Y. (2007). Mitochondria and peroxisomes: are the 'big brother' and the 'little sister' closer than assumed? *Bioessays* 29, 1105–1114. doi: 10.1002/bies.20659

Schulz, O., Pieper, C., Clever, M., Pfaff, J., Ruhlandt, A., Kehlenbach, R. H., et al. (2013). Resolution doubling in fluorescence microscopy with confocal spinning-disk image scanning microscopy. *Proc. Natl. Acad. Sci. U.S.A.* 110, 21000–21005. doi: 10.1073/pnas.1315858110

Schweizer, A., Fransen, J. A., Bachi, T., Ginsel, L., and Hauri, H. P. (1988). Identification, by a monoclonal antibody, of a 53-kD protein associated with a tubulo-vesicular compartment at the cis-side of the Golgi apparatus. *J. Cell Biol.* 107, 1643–1653. doi: 10.1083/jcb.107.5.1643

Scorrano, L., De Matteis, M. A., Emr, S., Giordano, F., Hajnoczky, G., Kornmann, B., et al. (2019). Coming together to define membrane contact sites. *Nat. Commun.* 10:1287. doi: 10.1038/s41467-019-09253-3

Sekar, R. B., and Periasamy, A. (2003). Fluorescence resonance energy transfer (FRET) microscopy imaging of live cell protein localizations. *J. Cell Biol.* 160, 629–633. doi: 10.1083/jcb.200210140

Severs, N. J., Jordan, E. G., and Williamson, D. H. (1976). Nuclear pore absence from areas of close association between nucleus and vacuole in synchronous yeast cultures. *J. Ultrastruct. Res.* 54, 374–387. doi: 10.1016/s0022-5320(76)80023-8

Sezgin, E. (2017). Super-resolution optical microscopy for studying membrane structure and dynamics. *J. Phys. Condens. Matter.* 29:273001. doi: 10.1088/1361-648X/aa7185

Shai, N., Yifrach, E., van Roermund, C. W. T., Cohen, N., Bibi, C., IJlst, L., et al. (2018). Systematic mapping of contact sites reveals tethers and a function for the peroxisome-mitochondria contact. *Nat. Commun.* 9:1761. doi: 10.1038/s41467-018-03957-8

Shaner, N. C., Campbell, R. E., Steinbach, P. A., Giepmans, B. N., Palmer, A. E., and Tsien, R. Y. (2004). Improved monomeric red, orange and yellow fluorescent proteins derived from Discosoma sp. red fluorescent protein. *Nat. Biotechnol.* 22, 1567–1572. doi: 10.1038/nbt1037

Shekhawat, S. S., and Ghosh, I. (2011). Split-protein systems: beyond binary protein-protein interactions. *Curr. Opin. Chem. Biol.* 15, 789–797. doi: 10.1016/j.cbpa.2011.10.014

Shim, S. H., Xia, C., Zhong, G., Babcock, H. P., Vaughan, J. C., Huang, B., et al. (2012). Super-resolution fluorescence imaging of organelles in live cells with photoswitchable membrane probes. *Proc. Natl. Acad. Sci. U.S.A.* 109, 13978–13983. doi: 10.1073/pnas.1201882109

Snapp, E. L., Hegde, R. S., Francolini, M., Lombardo, F., Colombo, S., Pedrazzini, E., et al. (2003). Formation of stacked ER cisternae by low affinity protein interactions. *J. Cell Biol.* 163, 257–269. doi: 10.1083/jcb.200306020

Soderberg, O., Gullberg, M., Jarvius, M., Ridderstrale, K., Leuchowius, K. J., Jarvius, J., et al. (2006). Direct observation of individual endogenous protein complexes in situ by proximity ligation. *Nat. Methods* 3, 995–1000. doi: 10.1038/nmeth947

Soderberg, O., Leuchowius, K. J., Gullberg, M., Jarvius, M., Weibrecht, I., Larsson, L. G., et al. (2008). Characterizing proteins and their interactions in cells and tissues using the in situ proximity ligation assay. *Methods* 45, 227–232. doi: 10.1016/j.ymeth.2008.06.014

Stefan, C. J., Trimble, W. S., Grinstein, S., Drin, G., Reinisch, K., De Camilli, P., et al. (2017). Membrane dynamics and organelle biogenesis-lipid pipelines and vesicular carriers. *BMC Biol.* 15:102. doi: 10.1186/s12915-017-0432-0

Stoica, R., De Vos, K. J., Paillusson, S., Mueller, S., Sancho, R. M., Lau, K. F., et al. (2014). ER-mitochondria associations are regulated by the VAPB-PTPIP51 interaction and are disrupted by ALS/FTD-associated TDP-43. *Nat. Commun.* 5:3996. doi: 10.1038/ncomms4996

Stoica, R., Paillusson, S., Gomez-Suaga, P., Mitchell, J. C., Lau, D. H., Gray, E. H., et al. (2016). ALS/FTD-associated FUS activates GSK-3beta to disrupt the VAPB-PTPIP51 interaction and ER-mitochondria associations. *EMBO Rep.* 17, 1326–1342. doi: 10.15252/embr.201541726

Subedi, K. P., Ong, H. L., Son, G. Y., Liu, X., and Ambudkar, I. S. (2018). STIM2 Induces Activated Conformation of STIM1 to Control Orai1 Function in ER-PM Junctions. *Cell Rep.* 23, 522–534. doi: 10.1016/j.celrep.2018.03.065

Swayne, T. C., Zhou, C., Boldogh, I. R., Charalel, J. K., McFaline-Figueroa, J. R., Thoms, S., et al. (2011). Role for cER and Mmr1p in anchorage of mitochondria at sites of polarized surface growth in budding yeast. *Curr. Biol.* 21, 1994–1999. doi: 10.1016/j.cub.2011.10.019

Sydor, A. M., Czymmek, K. J., Puchner, E. M., and Mennella, V. (2015). Super-resolution microscopy: from single molecules to supramolecular assemblies. *Trends Cell Biol.* 25, 730–748. doi: 10.1016/j.tcb.2015.10.004

Szabadkai, G., Bianchi, K., Varnai, P., De Stefani, D., Wieckowski, M. R., Cavagna, D., et al. (2006). Chaperone-mediated coupling of endoplasmic reticulum and mitochondrial Ca^{2+} channels. *J. Cell Biol.* 175, 901–911. doi: 10.1083/jcb.200608073

Takeshima, H., Komazaki, S., Nishi, M., Iino, M., and Kangawa, K. (2000). Junctophilins: a novel family of junctional membrane complex proteins. *Mol. Cell* 6, 11–22. doi: 10.1016/s1097-2765(00)00003-4

Thomas, H. E., Zhang, Y., Stefely, J. A., Veiga, S. R., Thomas, G., Kozma, S. C., et al. (2018). Mitochondrial complex I activity is required for maximal autophagy. *Cell Rep.* 24, 2404–2417.e8. doi: 10.1016/j.celrep.2018.07.101

Toulmay, A., and Prinz, W. A. (2012). A conserved membrane-binding domain targets proteins to organelle contact sites. *J. Cell. Sci.* 125(Pt 1), 49–58. doi: 10.1242/jcs.085118

Tubbs, E., and Rieusset, J. (2016). Study of endoplasmic reticulum and mitochondria interactions by *in situ* proximity ligation assay in fixed cells. *J. Vis. Exp.* 118:54899. doi: 10.3791/54899

Valm, A. M., Cohen, S., Legant, W. R., Melunis, J., Hershberg, U., Wait, E., et al. (2017). Applying systems-level spectral imaging and analysis to reveal the organelle interactome. *Nature* 546, 162–167. doi: 10.1038/nature22369

van Vliet, A. R., Giordano, F., Gerlo, S., Segura, I., Van Eygen, S., Molenberghs, G., et al. (2017). The ER Stress Sensor PERK Coordinates ER-Plasma Membrane Contact Site Formation through Interaction with Filamin-A and F-Actin Remodeling. *Mo. Cell* 65 88, 885–899.e6. doi: 10.1016/j.molcel.2017.01.020

Vance, J. E., Stone, S. J., and Faust, J. R. (1997). Abnormalities in mitochondria-associated membranes and phospholipid biosynthetic enzymes in the mnd/mnd mouse model of neuronal ceroid lipofuscinosis. *Biochim. Biophys. Acta* 1344, 286–299. doi: 10.1016/s0005-2760(96)00153-1

Wang, H., Becuwe, M., Housden, B. E., Chitraju, C., Porras, A. J., Graham, M. M., et al. (2016). Seipin is required for converting nascent to mature lipid droplets. *eLife* 5:e16582. doi: 10.7554/eLife.16582

Wang, H., Sreenivasan, U., Hu, H., Saladino, A., Polster, B. M., Lund, L. M., et al. (2011). Perilipin 5, a lipid droplet-associated protein, provides physical and metabolic linkage to mitochondria. *J. Lipid Res.* 52, 2159–2168. doi: 10.1194/jlr.M017939

Wiens, M. D., and Campbell, R. E. (2018). Surveying the landscape of optogenetic methods for detection of protein-protein interactions. *Wiley Interdiscip. Rev. Syst. Biol. Med.* 10:e1415. doi: 10.1002/wsbm.1415

Wijdeven, R. H., Janssen, H., Nahidiazar, L., Janssen, L., Jalink, K., Berlin, I., et al. (2016). Cholesterol and ORP1L-mediated ER contact sites control autophagosome transport and fusion with the endocytic pathway. *Nat. Commun.* 7:11808. doi: 10.1038/ncomms11808

Wong, Y. C., Ysselstein, D., and Krainc, D. (2018). Mitochondria-lysosome contacts regulate mitochondrial fission via RAB7 GTP hydrolysis. *Nature* 554, 382–386. doi: 10.1038/nature25486

Wouters, F. S., Bastiaens, P. I., Wirtz, K. W., and Jovin, T. M. (1998). FRET microscopy demonstrates molecular association of non-specific lipid transfer protein (nsL-TP) with fatty acid oxidation enzymes in peroxisomes. *EMBO J.* 17, 7179–7189. doi: 10.1093/emboj/17.24.7179

Wu, Y., Whiteus, C., Xu, C. S., Hayworth, K. J., Weinberg, R. J., Hess, H. F., et al. (2017). Contacts between the endoplasmic reticulum and other membranes in neurons. *Proc. Natl. Acad. Sci. U.S.A.* 114, E4859–E4867. doi: 10.1073/pnas.1701078114

Xu, D., Li, Y., Wu, L., Li, Y., Zhao, D., Yu, J., et al. (2018). Rab18 promotes lipid droplet (LD) growth by tethering the ER to LDs through SNARE and NRZ interactions. *J. Cell Biol.* 217, 975–995. doi: 10.1083/jcb.201704184

Xu, N., Zhang, S. O., Cole, R. A., McKinney, S. A., Guo, F., Haas, J. T., et al. (2012). The FATP1-DGAT2 complex facilitates lipid droplet expansion at the ER-lipid droplet interface. *J. Cell Biol.* 198, 895–911. doi: 10.1083/jcb.201201139

Xue, M., Hou, J., Wang, L., Cheng, D., Lu, J., Zheng, L., et al. (2017). Optimizing the fragment complementation of APEX2 for detection of specific protein-protein interactions in live cells. *Sci. Rep.* 7:12039. doi: 10.1038/s41598-017-12365-9

Yamamoto, K., and Fahimi, H. D. (1987). Three-dimensional reconstruction of a peroxisomal reticulum in regenerating rat liver: evidence of interconnections between heterogeneous segments. *J. Cell Biol.* 105, 713–722. doi: 10.1083/jcb.105.2.713

Yang, Z., Zhao, X., Xu, J., Shang, W., and Tong, C. (2018). A novel fluorescent reporter detects plastic remodeling of mitochondria-ER contact sites. *J. Cell Sci.* 131:jcs208686. doi: 10.1242/jcs.208686

Youn, J. Y., Dunham, W. H., Hong, S. J., Knight, J. D. R., Bashkurov, M., Chen, G. I., et al. (2018). High-density proximity mapping reveals the subcellular organization of mRNA-associated granules and bodies. *Mol. Cell* 69, 517–532.e11. doi: 10.1016/j.molcel.2017.12.020

Zhanghao, K., Chen, X., Liu, W., Li, M., Liu, Y., Wang, Y., et al. (2019). Super-resolution imaging of fluorescent dipoles via polarized structured illumination microscopy. *Nat. Commun.* 10:4694. doi: 10.1038/s41467-019-12681-w

Zimmer, M. (2002). Green fluorescent protein (GFP): applications, structure, and related photophysical behavior. *Chem. Rev.* 102, 759–781.

Conflict of Interest: The authors declare that the research was conducted in the absence of any commercial or financial relationships that could be construed as a potential conflict of interest.

Copyright © 2020 Huang, Jiang, Yu and Yang. This is an open-access article distributed under the terms of the Creative Commons Attribution License (CC BY). The use, distribution or reproduction in other forums is permitted, provided the original author(s) and the copyright owner(s) are credited and that the original publication in this journal is cited, in accordance with accepted academic practice. No use, distribution or reproduction is permitted which does not comply with these terms.